

Looking for $z>7$ star-forming galaxies in lensing fields

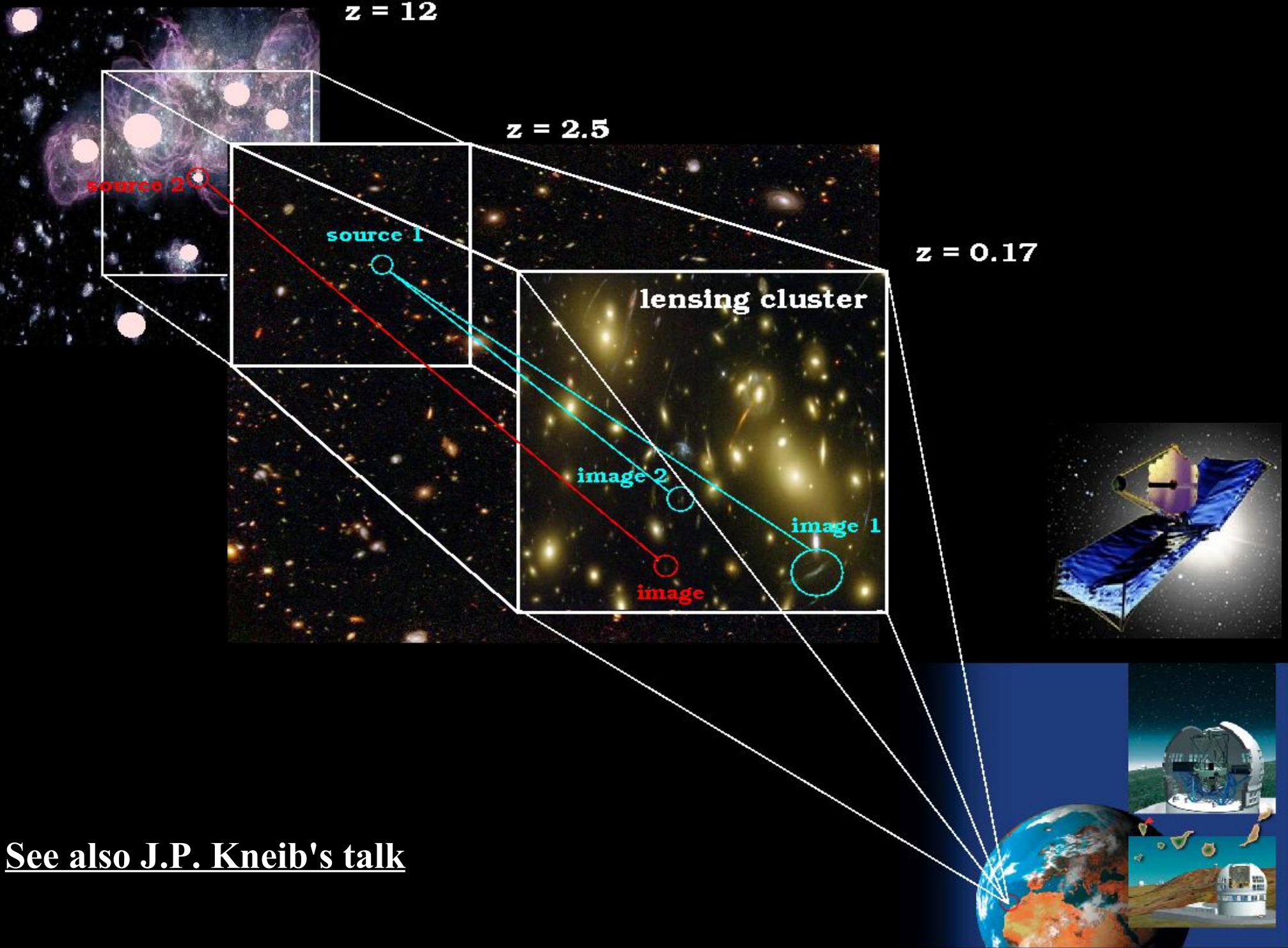
Roser Pelló

LATT - Laboratoire d'Astrophysique de Toulouse-Tarbes

J. Richard (Caltech) - A. Maizy (LATT)

*D. Schaefer (O. Genève), A. Hempel (IAC)-J.F. Le Borgne (LATT) -
J. P. Kneib (LAM, Marseille)- E. Egami (Tucson) - M. Wise
(MIT/NL) - F. Boone, F. Combes (O. Paris) - A. Ferrara (Trieste) -
M.A. De Leo (UNAM) & the GOYA collaboration*





See also J.P. Kneib's talk

Outline:

1. Designing future “massive” spectroscopic surveys targeting $z > \sim 7$ galaxies: a matter of efficiency.

- Lensing or blank fields?
- Towards an « ideal » combination of lensing clusters and blank fields.

See also A. Maizy's poster

2. Back to real life: A multi-wavelength survey of distant galaxies ($z > \sim 7$) with Gravitational Telescopes.

- Project design, results and problems.
- Spectroscopic follow-up and multi-wavelength analysis.

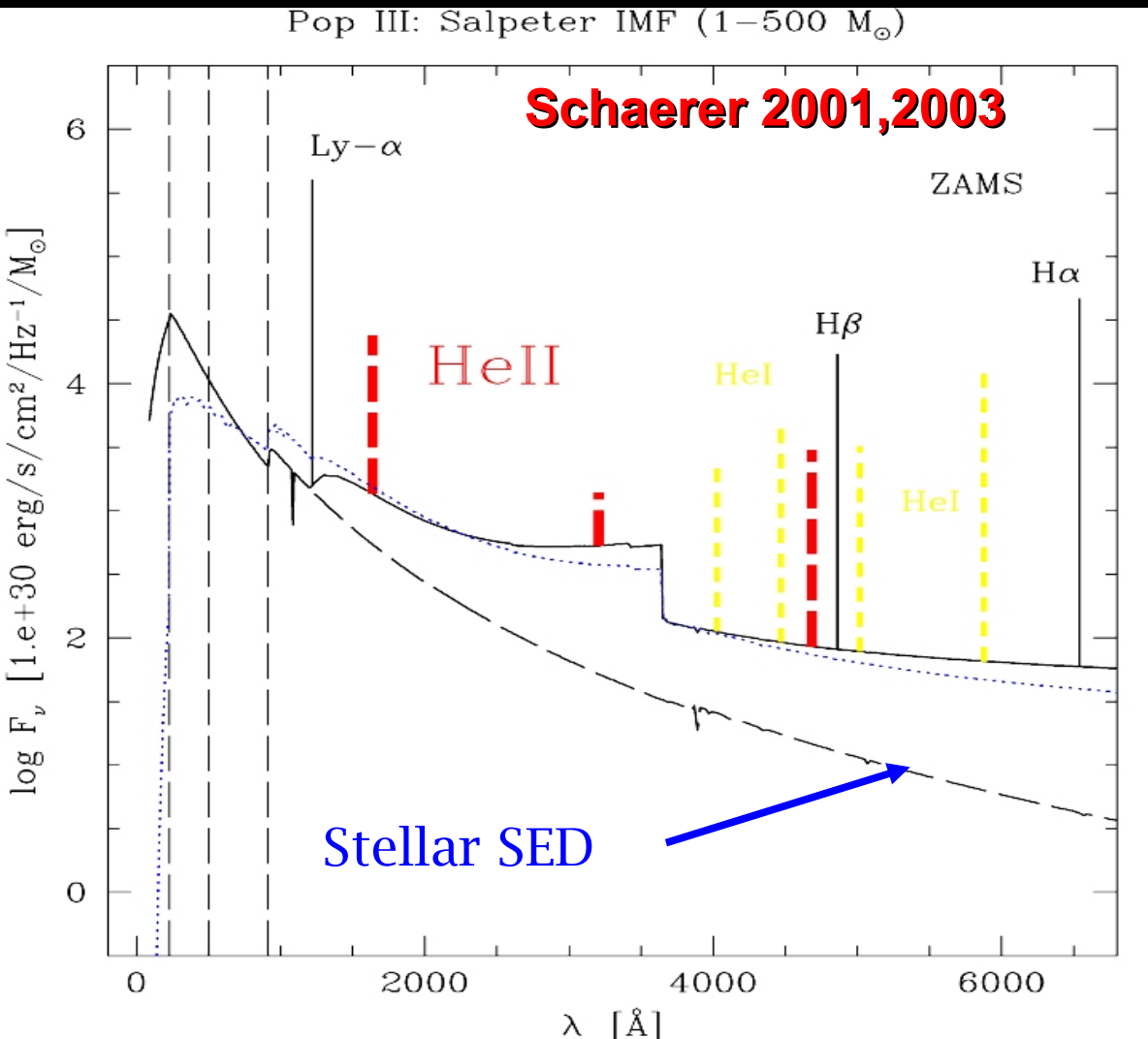


Designing future “massive”
spectroscopic surveys targeting
 $z > \sim 7$ galaxies:

A matter of efficiency

Spectroscopic Observations

- Determination redshift and nature of sources
- Studying the physical properties of the firsts starbursts



- *SFR*
 - *LFs ==> reionization*
 - *Stellar populations*
 - *PopIII starbursts?*
 - Top - heavy IMF
 - Very massive stars, up to ~500-1000 M_{\odot}
- Nebular continuous emission dominates the spectrum at $\lambda > 1400 \text{ \AA}$
- + Strong Hell lines?: Hell $\lambda 1640$. Hell $\lambda 3203$. Hell

See D. Scherer's talk

A new generation of near-IR spectrographs

- Near-IR multi-object capabilities (~20 to 60 targets) in 10m class telescopes
- Large FOV (~4' to 6' wide)
- Optimal spectral resolution: R~3000 to 6000 (large sky-free wavelength coverage)
- “Deep” Spectroscopic follow up from the ground (JWST synergy).

An example: EMIR/ GTC



EMIR/GOYA Survey
(~2010):

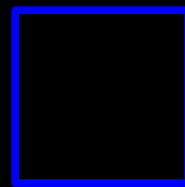
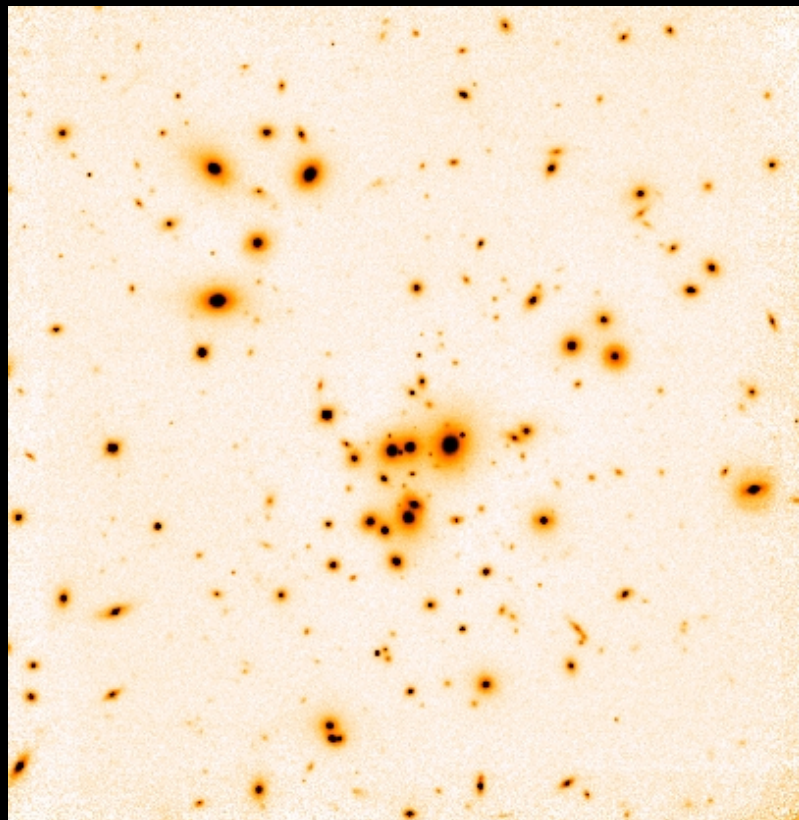
Other examples:

MOIRCS/Subaru (in HR mode)
– Flamingos2/Gemini-S –
KMOS/VLT 2nd generation



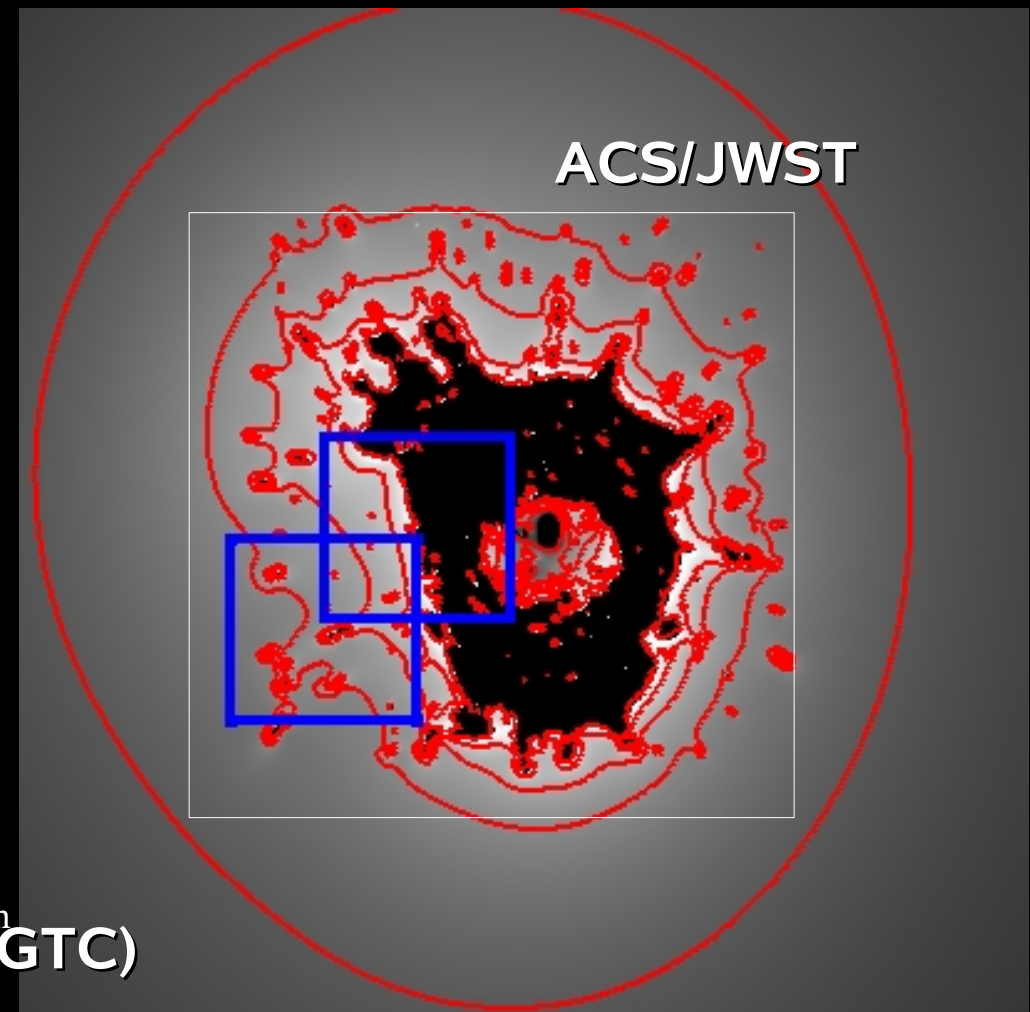
<http://www.astro.ufl.edu/GOYA/home.html>

Blank Fields versus lensing fields

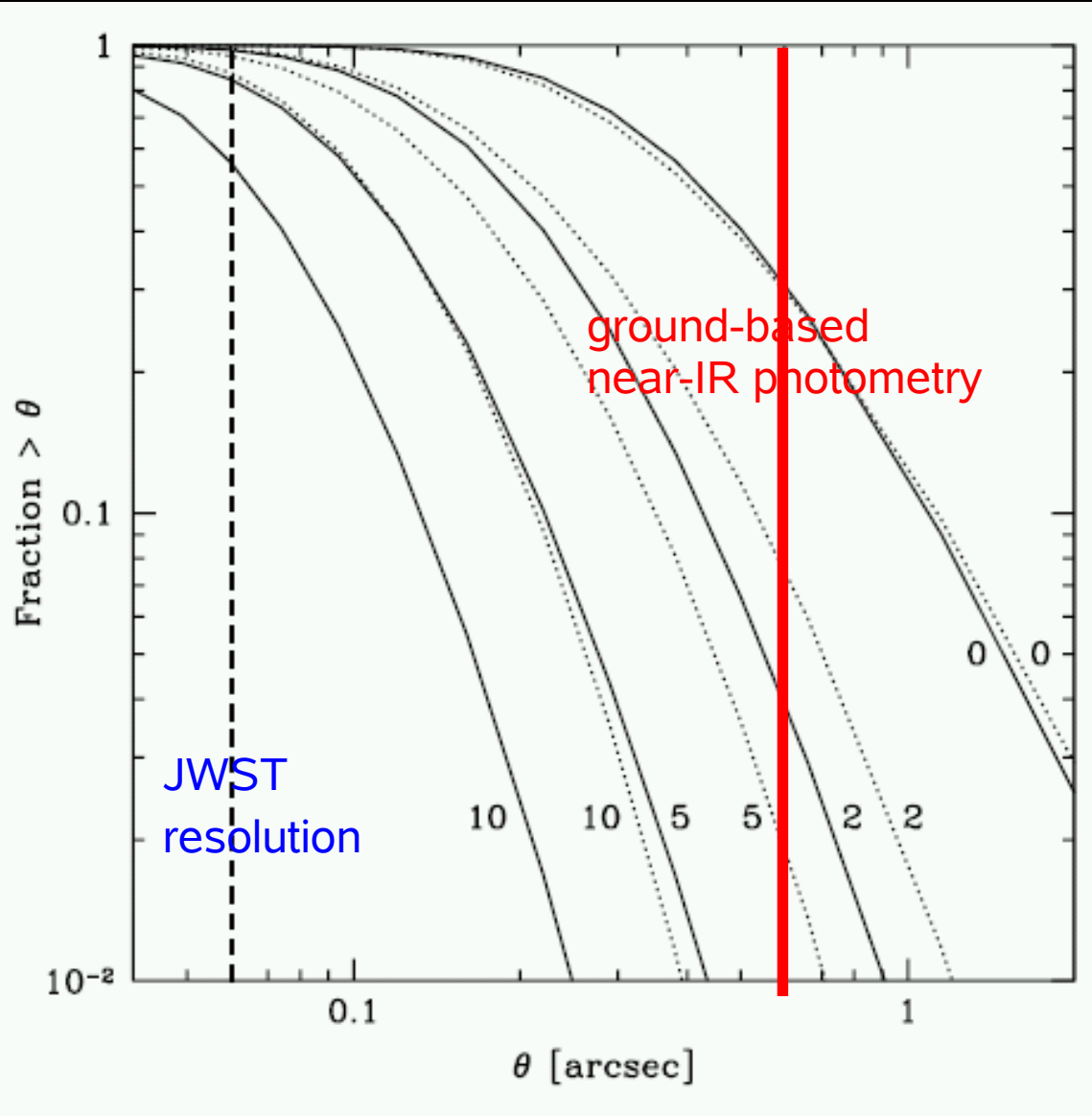


FOV (1'x1')
NICMOS-NIC3

- Example: A1689 ($z(\text{cluster})=0.184$)
- Lenstool modeling of cluster mass distribution
- Magnification ($z(\text{source})=6$): 2, 5, 10, 25

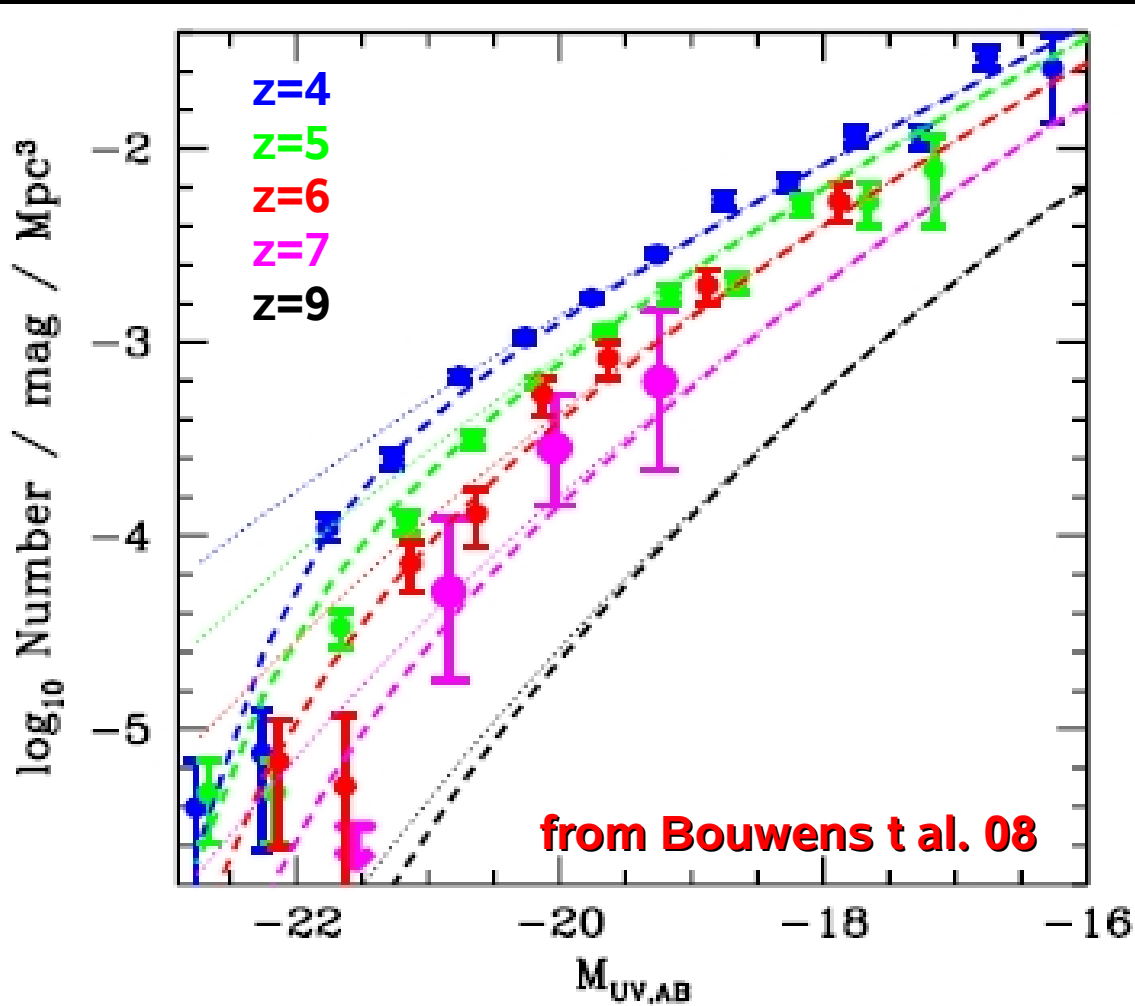


Blank Fields versus lensing fields



- Distribution of disk sizes in Λ CDM model.
- Diameter measured out to one exponential scale length.
- Limiting point-like source flux of 1nJy.
- Most $z \sim 10$ sources are expected to remain non-resolved, even with a magnification factor $\mu \sim 10$.

Deriving Expected Number counts



- Deriving expected number counts from realistic/observed UV LFs at $6 < z < 12$.
- Comparison between expected $N(z,m)$ in blank & lensing fields
- Pixel-to-pixel integration of magnification maps, using lensing models and bright-objects masking.

$$\langle z \rangle = 4.0$$

$$\alpha = 1.6,$$

$$\phi^* = 1.3 \cdot 10^{-2} \text{ Mpc}^{-3},$$

$$M^* = -21.07$$

Steidel et al. (1999)

$$\langle z \rangle = 5.9$$

$$\alpha = 1.74,$$

$$\phi^* = 1.1 \cdot 10^{-3} \text{ Mpc}^{-3},$$

$$M^* = -20.24$$

Bouwens et al. (2006)

$$3.8 < z < 7.4$$

$$\alpha = 1.74,$$

$$\phi^* = 1.1 \cdot 10^{-3} \text{ Mpc}^{-3},$$

$$M^* = -21.02 + 0.36(z - 3.8)$$

Bouwens et al. (2008)

Deriving Expected Number counts

- 2 opposite lensing effects:

magnification ($\mu(z)$)

and dilution ($1/\mu(z)$):

$$N_{\text{lensing}}(>L, z) = N(>L/\mu, z) / \mu(z)$$

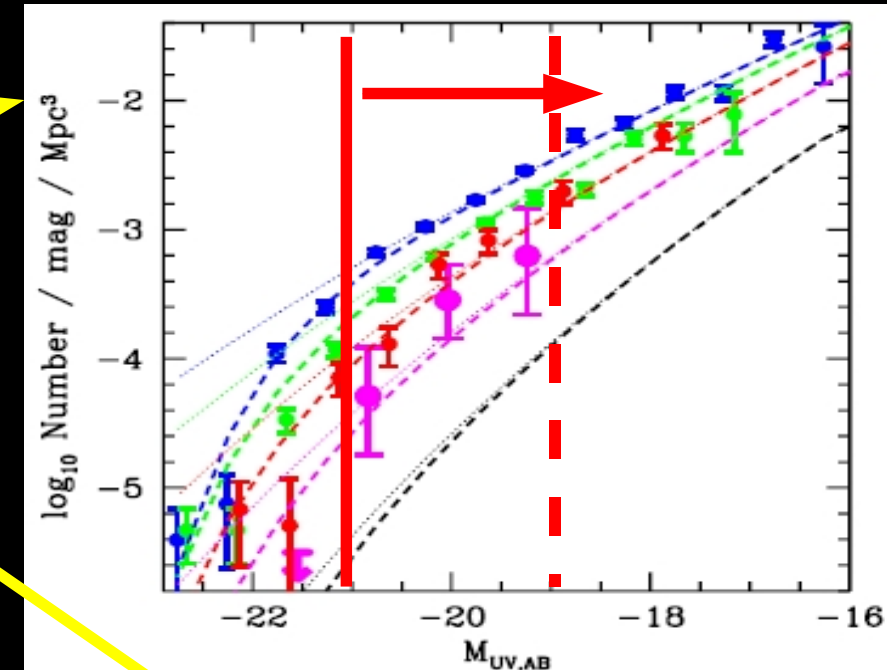
- Positive/negative magnification bias (e.g. Broadhurst et al. 95):

$$N_{\text{lensed}}(> L) = N(> L) \times \mu^{\alpha-1}$$

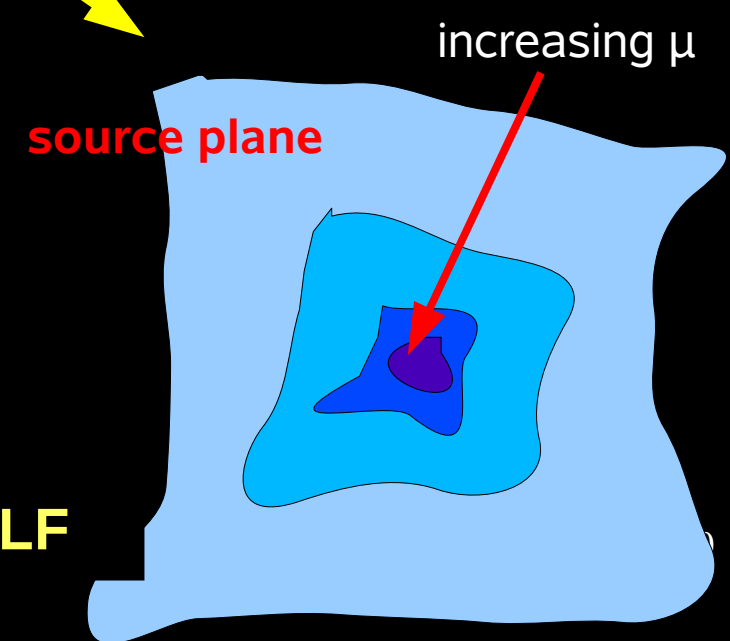
$$\alpha = -d(\log n)/d(\log L)$$

i.e. $\alpha > 1 \Rightarrow N(\text{lensing}) > N(\text{blank field})$

Number counts are highly sensitive to α
 ==> comparison between $N(\text{lensing})$ and
 $N(\text{blank})$ helps constraining the faint end of LF



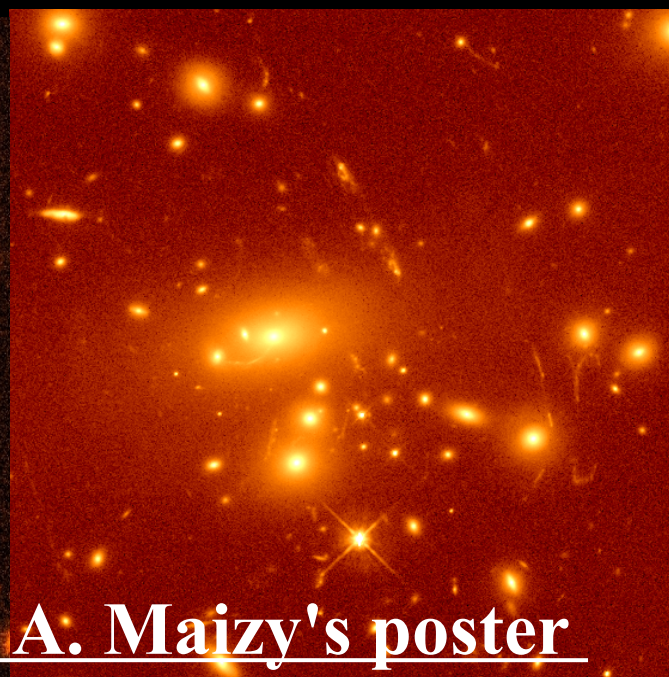
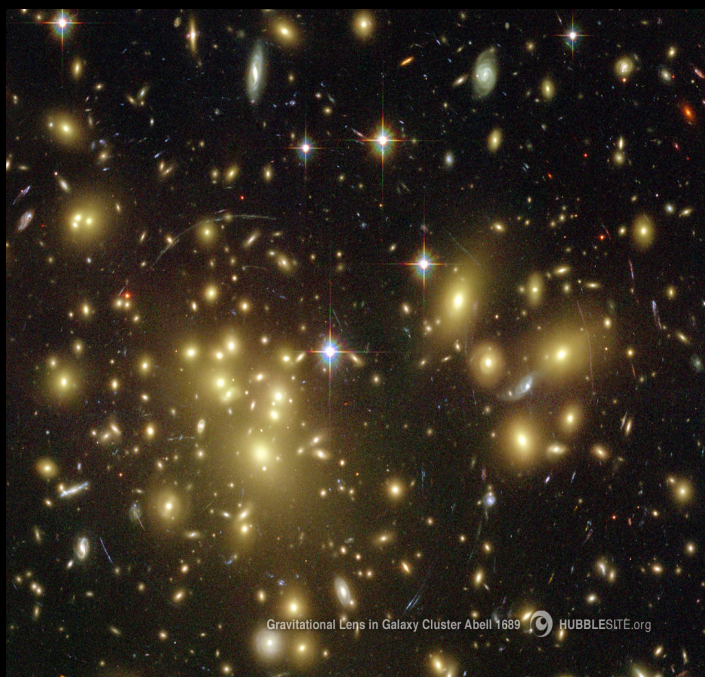
with



Deriving Expected Number counts

- 3 “reference” lensing clusters: A1689 ($z=0.184$), A1835 ($z=0.25$), and AC114 ($z=0.310$)
- *Lenstool* lensing models
 - *cluster scale mass component*
 - *galaxy scale mass component*

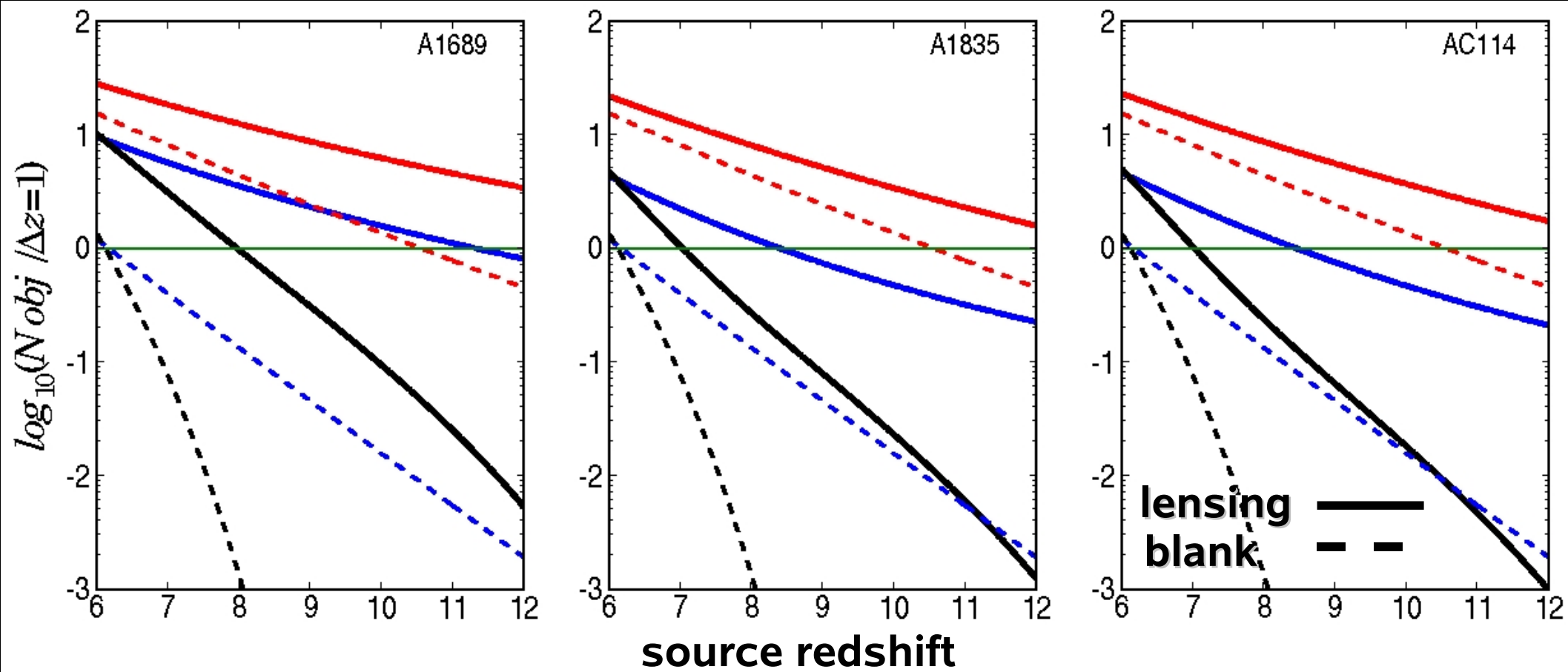
| | A1689 | A1835 | AC114 |
|-------------------------|---------|---------|---------|
| Large scale components | | | |
| r_{core} kpc | 90.02 | 50.00 | 97.04 |
| r_{cut} kpc | 1930.35 | 1000.00 | 2226.30 |
| v_{disp} km/s | 1334.31 | 1210.00 | 1035.98 |
| z_c | 0.184 | 0.253 | 0.310 |
| Number of substructures | 266 | 90 | 28 |



See also A. Maizy's poster

Blank Fields versus lensing fields

« Bright » spectroscopic sample: $H(AB) < \sim 25.5$ in a $6' \times 6'$ FOV, $\Delta z = 1$



$$\langle z \rangle = 4.0 \quad \alpha = 1.6, \quad \phi^* = 1.3 \cdot 10^{-2} \text{ Mpc}^{-3}, \quad M^* = -21.07$$

Steidel et al. (1999)

$$\langle z \rangle = 5.9 \quad \alpha = 1.74, \quad \phi^* = 1.1 \cdot 10^{-3} \text{ Mpc}^{-3}, \quad M^* = -20.24$$

Bouwens et al. (2006)

$$3.8 < z < 7.4 \quad \alpha = 1.74, \quad \phi^* = 1.1 \cdot 10^{-3} \text{ Mpc}^{-3}, \quad M^* = -21.02 + 0.36(z - 3.8)$$

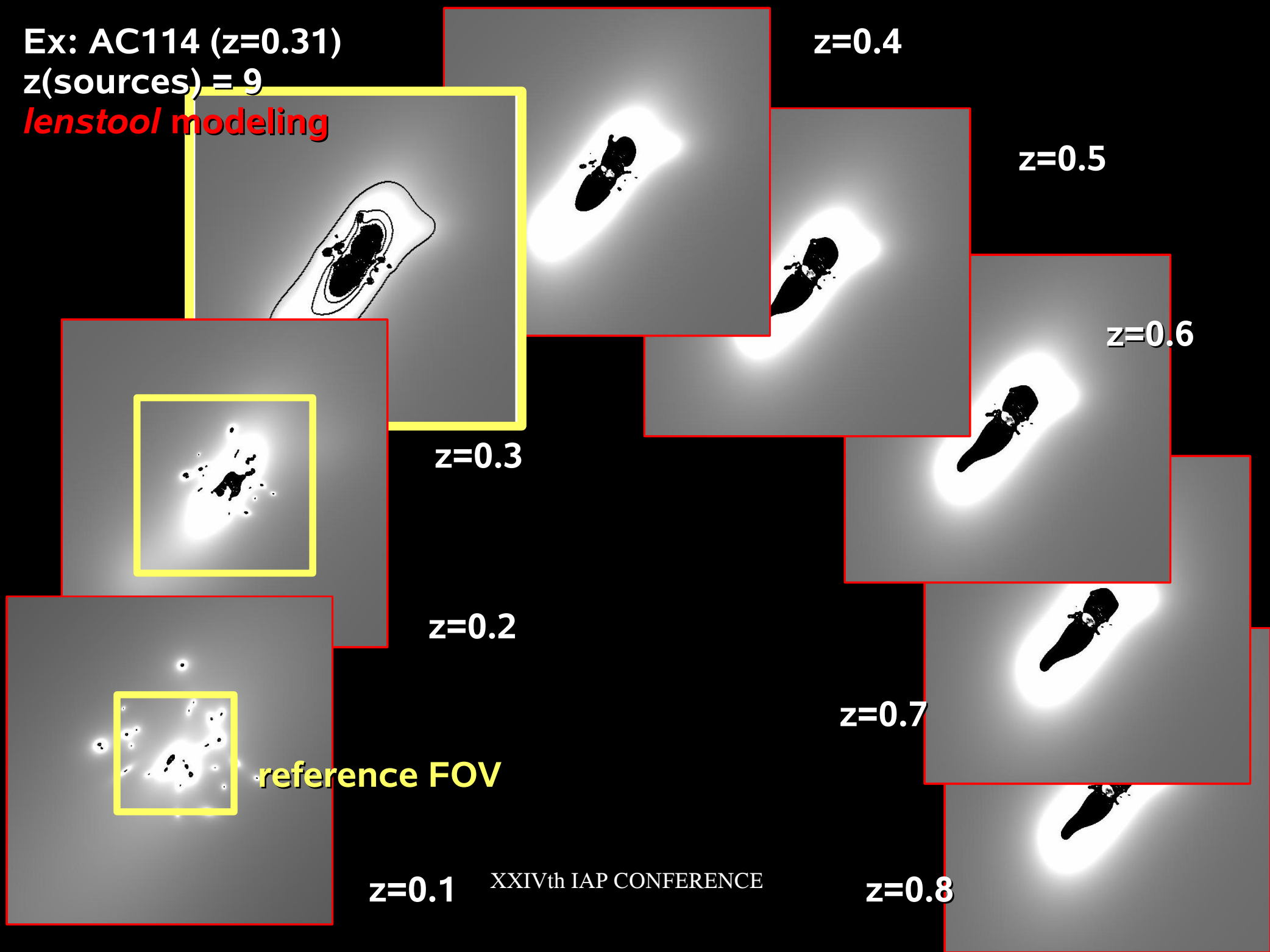
Bouwens et al. (2008)

See also A. Maizy's poster

Ex: AC114 ($z=0.31$)

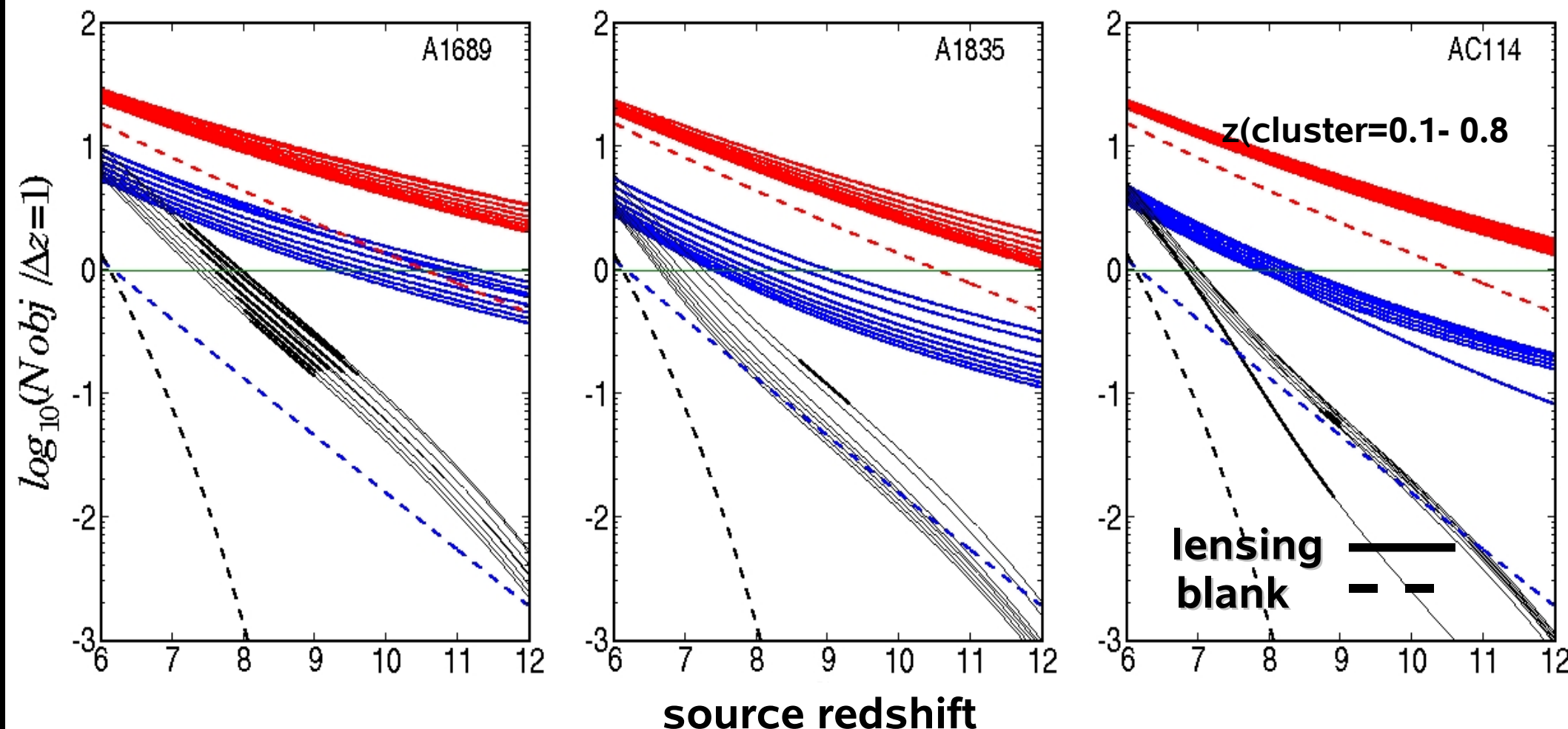
$z(\text{sources}) = 9$

lenstool modeling



Blank Fields versus lensing fields

« Bright » spectroscopic sample: $H(AB) < \sim 25.5$ in a $6' \times 6'$ FOV, $\Delta z = 1$



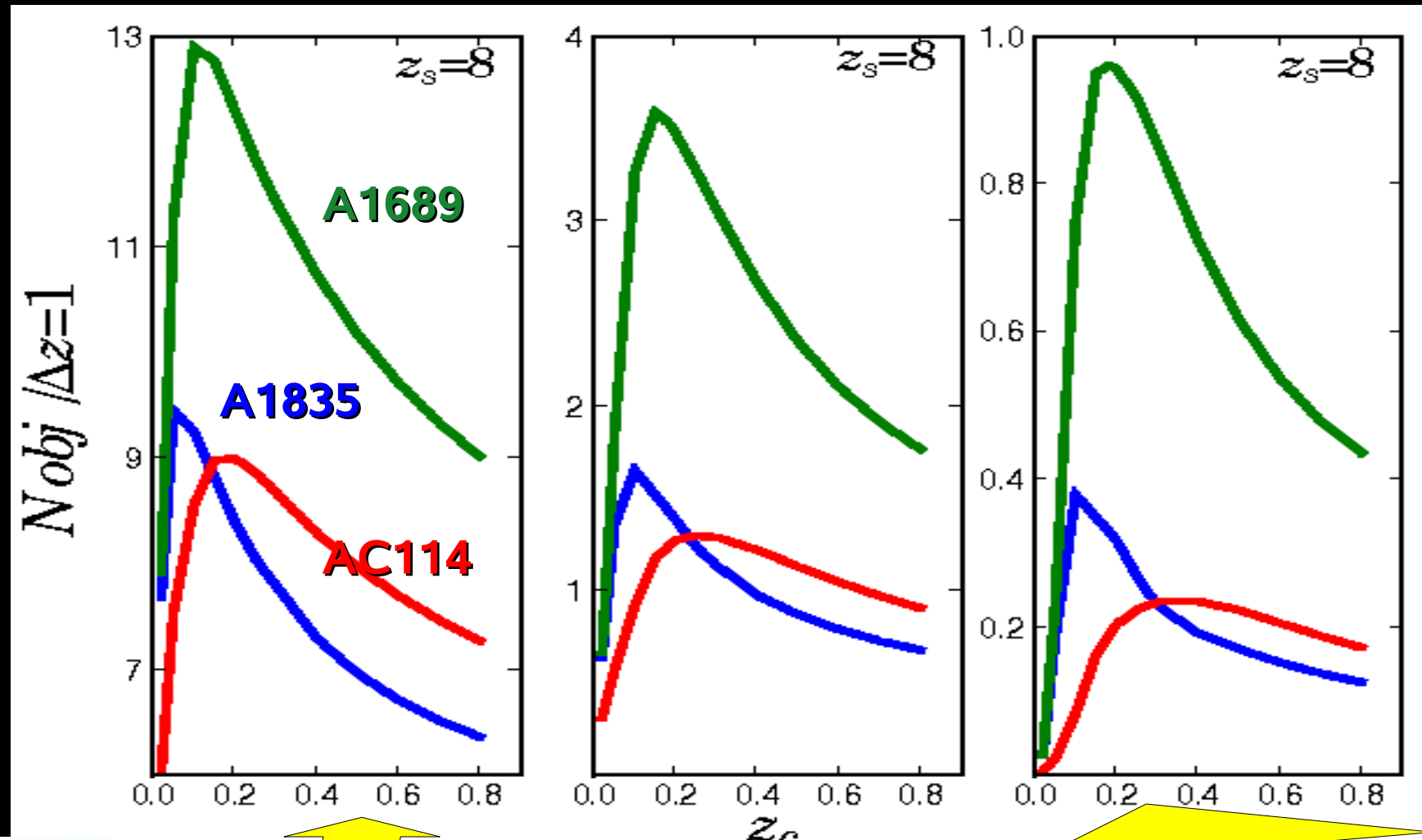
Steidel et al. (1999)

Bouwens et al. (2006)

Bouwens et al. (2008)

Blank Fields versus lensing fields

« Bright » spectroscopic sample: $H(AB) < \sim 25.5$ in a $6' \times 6'$ FOV, $\Delta z=1$



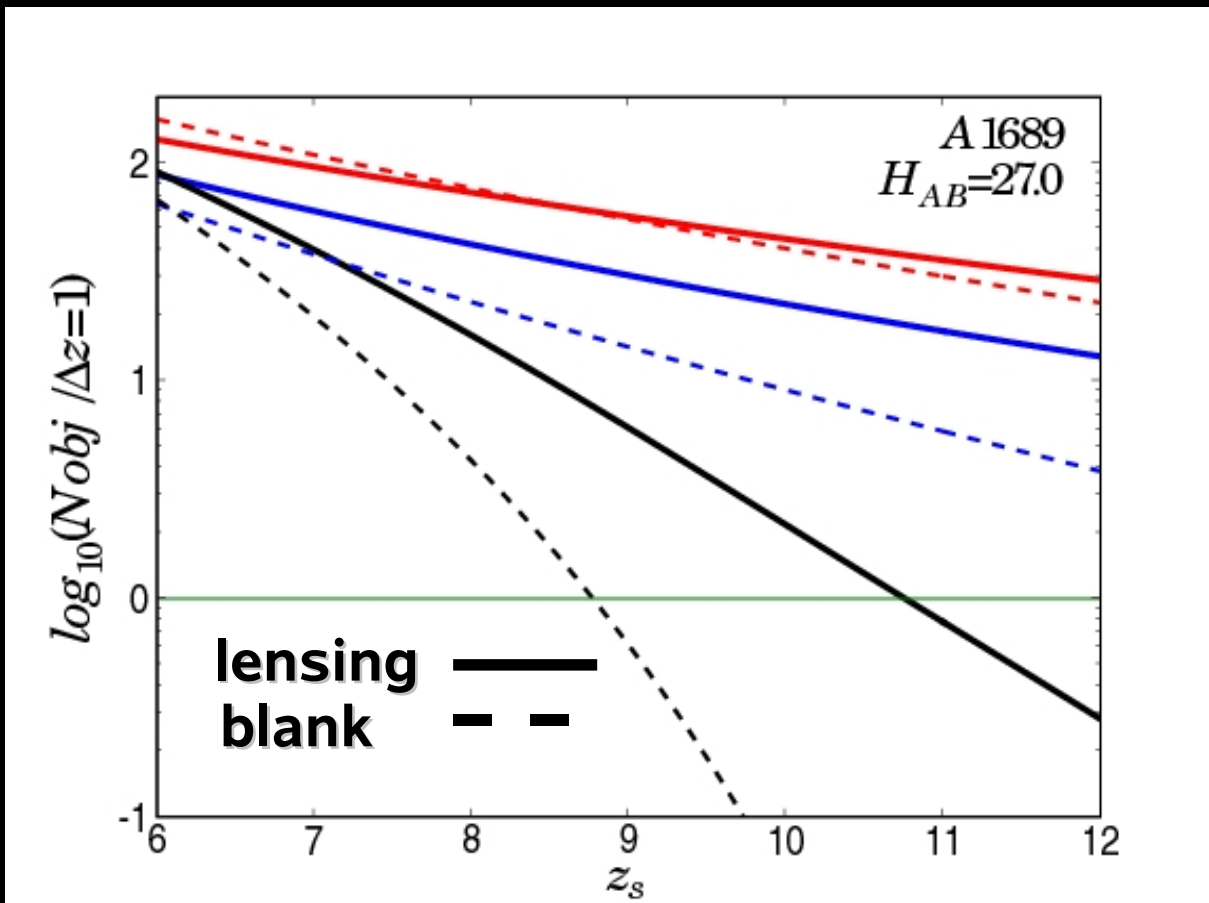
Steidel et al. (1999)

Bouwens et al. (2006)

Bouwens et al. (2008)

Blank Fields versus lensing fields

« Faint » photometric sample: $H(\text{AB}) < \sim 27.0$ in a $6' \times 6'$ FOV, $\Delta z=1$



- A lensing cluster along the line of sight has an increasingly positive influence on observation efficiency for:
 - “shallow” surveys
 - strongly evolving LFs
 - increasing with z(sources)

Steidel et al. (1999)

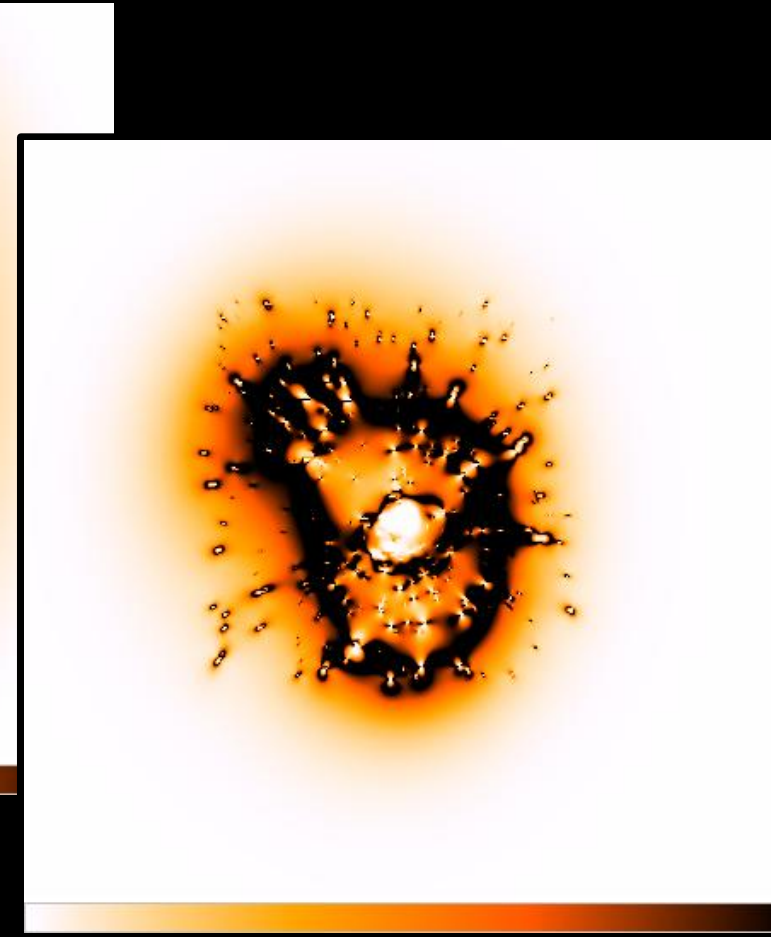
Bouwens et al. (2006)

Bouwens et al. (2008)

Towards an “ideal” survey

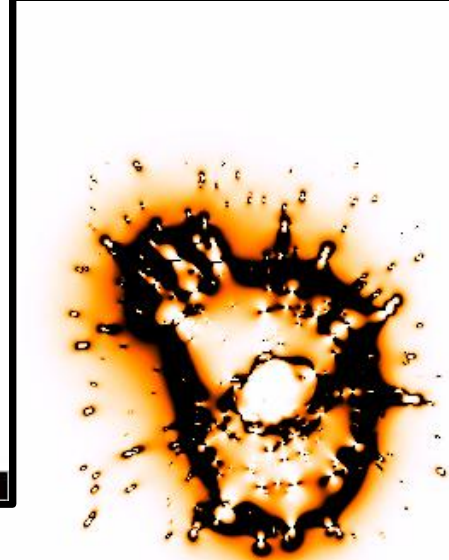
Probability density in lensing clusters: ex. A1689, 6' x 6' FOV,
magnitude limited sample

$z=6$



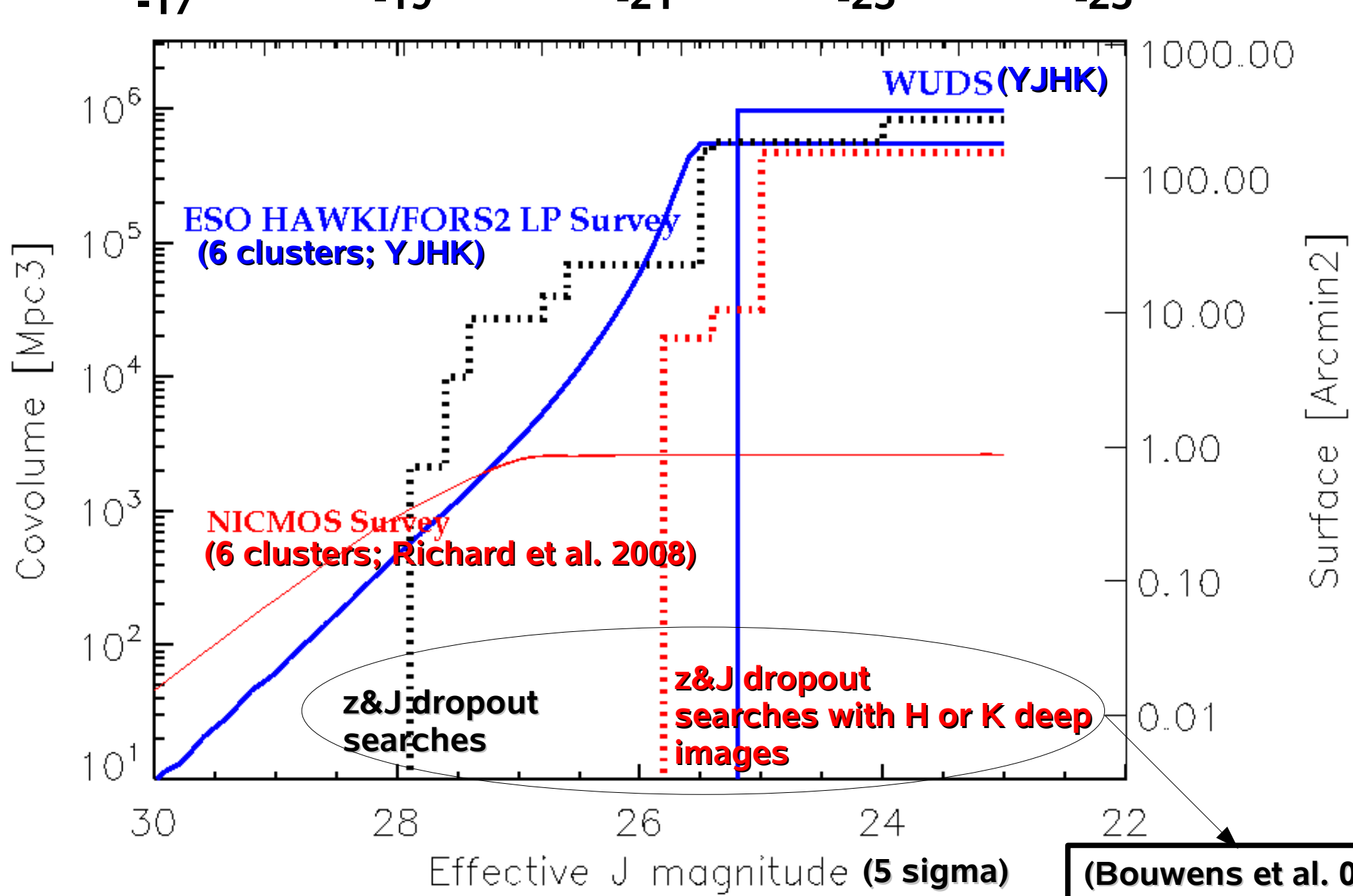
$z=8$

$z=10$



$z \sim 7-8.5$

M_AB (1500A)





**Back to real life:
A multi-wavelength survey of
distant galaxies ($z > \sim 7$) with
Gravitational Telescopes**

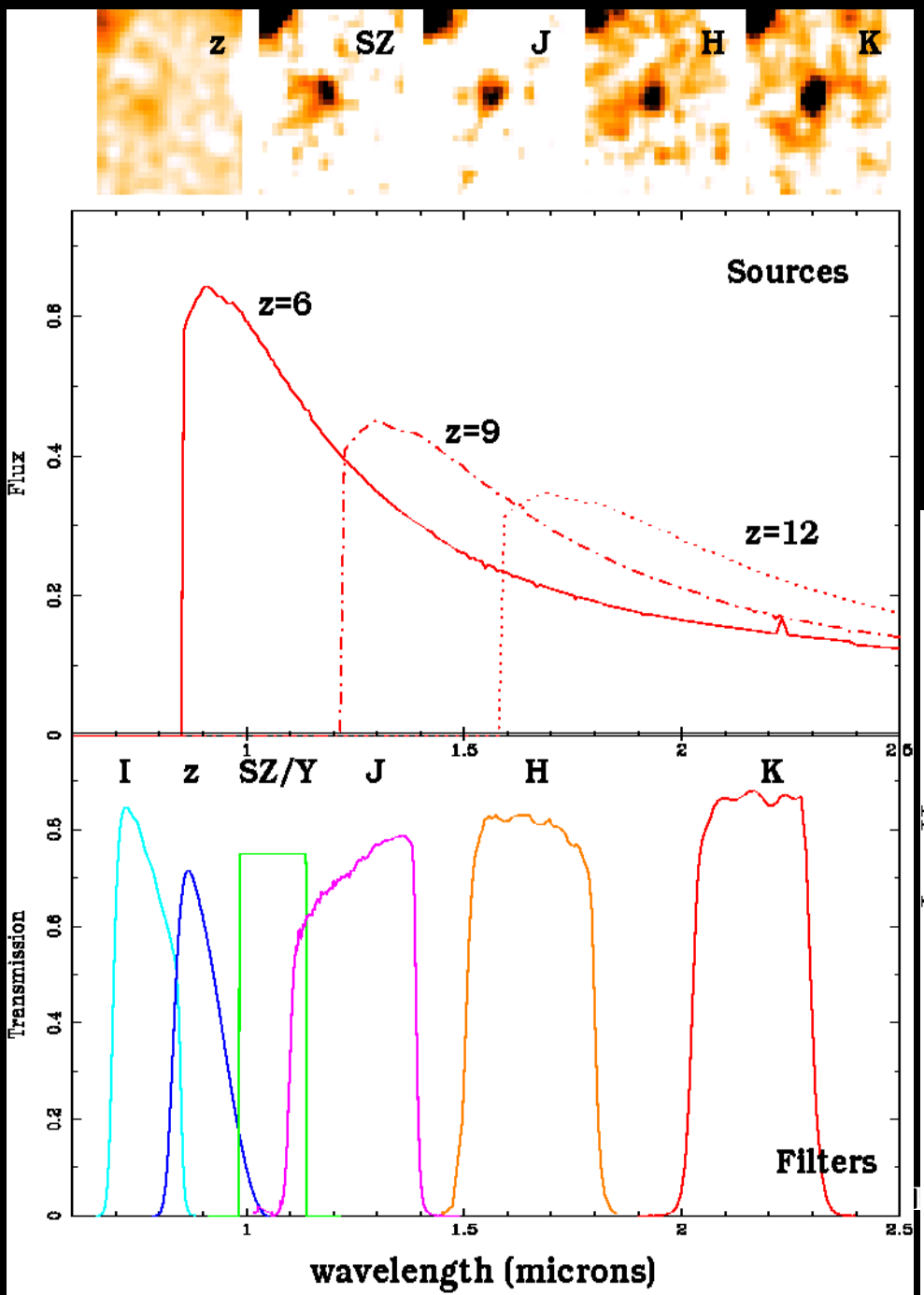
Project Design

- **2001 ---> SpectroPhotometric Simulations:**
 - Broad-band colors for “drop-out” selection at various redshifts ($z \sim 6-7$, $z \sim 7-8$, $z \sim 8-12$).
 - Expected magnitudes for normal, low metallicity, and PopIII starbursts with different IMF, SF histories.
 - Feasibility studies: lensing vs. blank fields; pilot studies for the new generation of near-IR instruments .
- **2002 ---> Deep near-IR (JHK, SZ) Imaging of well studied lensing clusters with ISAAC/VLT combined with deep optical imaging, including HST imaging.**
- **2003 ---> High-z Candidate Selection. Different detection criteria. Exploitation of final H-band selected sample.**
- **2003/04 ---> Pilot Spectroscopic Follow-up of best candidates ISAAC/VLT.**
- **2005/06 ---> Multi-wavelength follow up (Spitzer-IRAC, Chandra, IRAM, ...)**

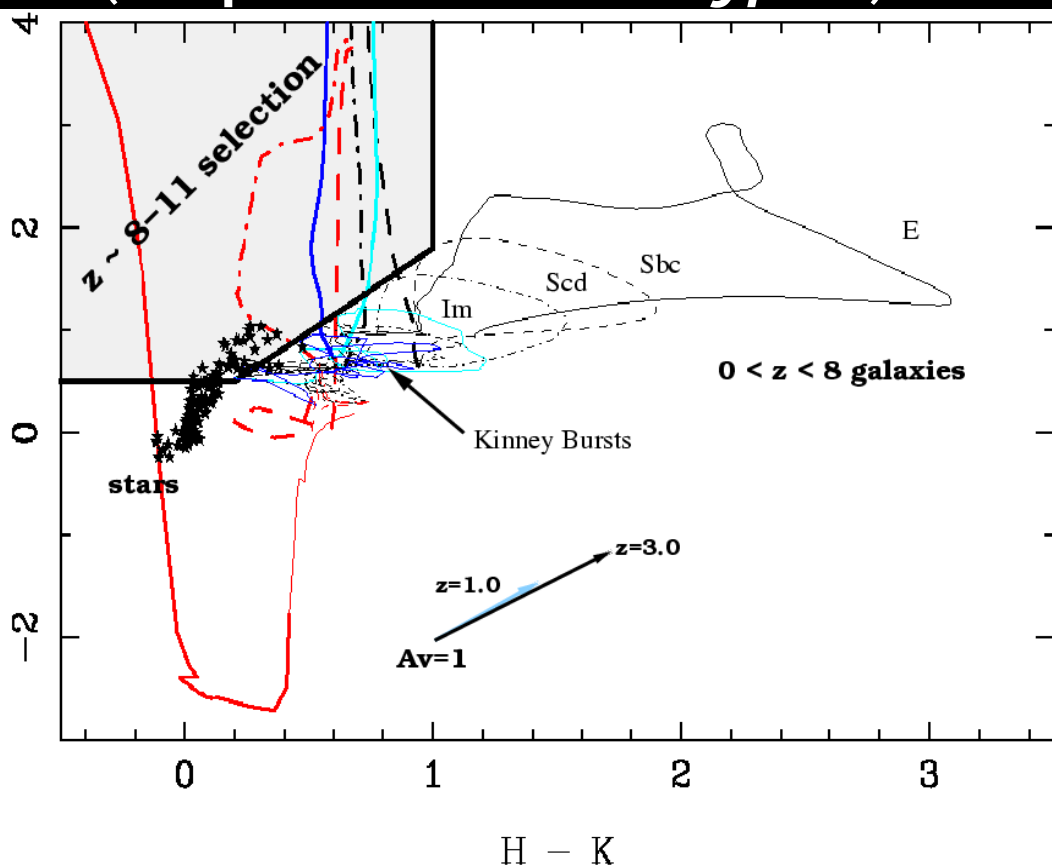


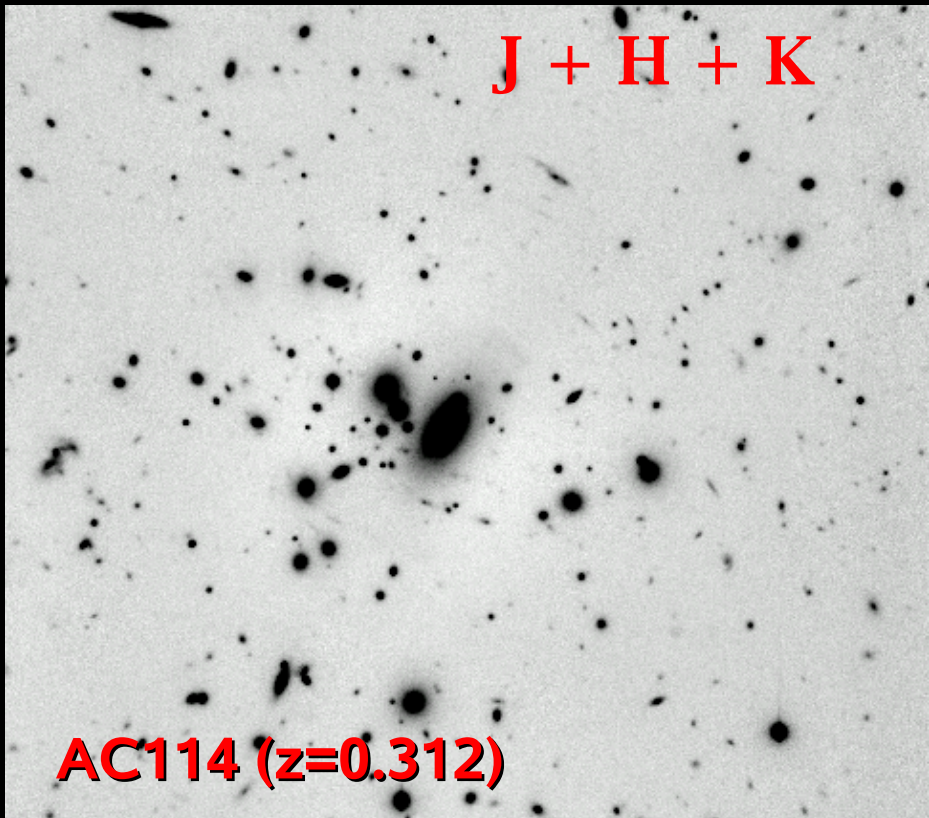
Next generation of multi-object near-IR spectrographs

Selection of photometric candidates



- Optical dropouts + near-IR colors
- Filter combinations:
 - $z \sim 6-7$: zYJ
 - $z \sim 7-8$: YJH
 - $z \sim 8-12$: JHK
- SED-fitting and photo-zs
(adapted version of *Hyperz*)





ISaac/VLT photometry (Vega system, 3σ):

J : 2h (J = 24.3)

H : 4h (H = 23.5)

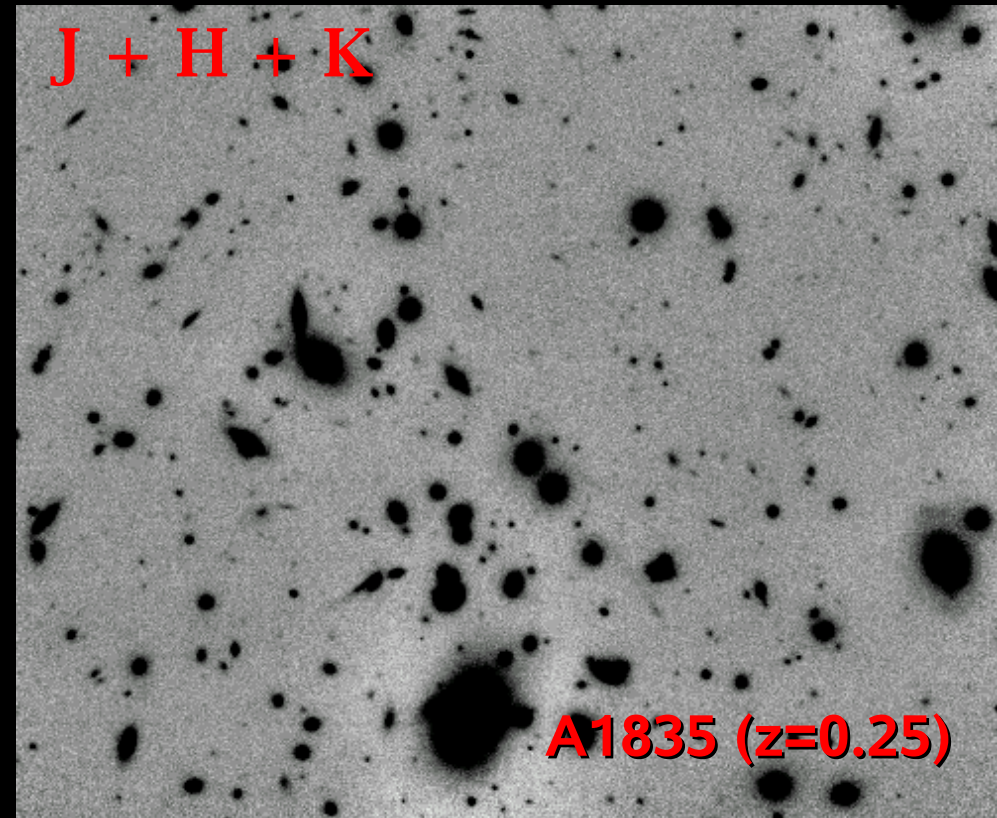
K': 5.5 h (K' = 23.2 --> K(AB)~25.0)

seeing ~0.4-0.6"

+ UBVRI Optical data + HST R band

+ ACS/F850W (~28 AB) + FORS (V~28 AB, 3 σ) + NIRI (H~26 AB, 3 σ)

+ HST/NICMOS (1 pointing/cluster) + IRAC/SPITZER new data



ISaac/VLT photometry (Vega system, 3σ):

J : 2h (J = 24.4)

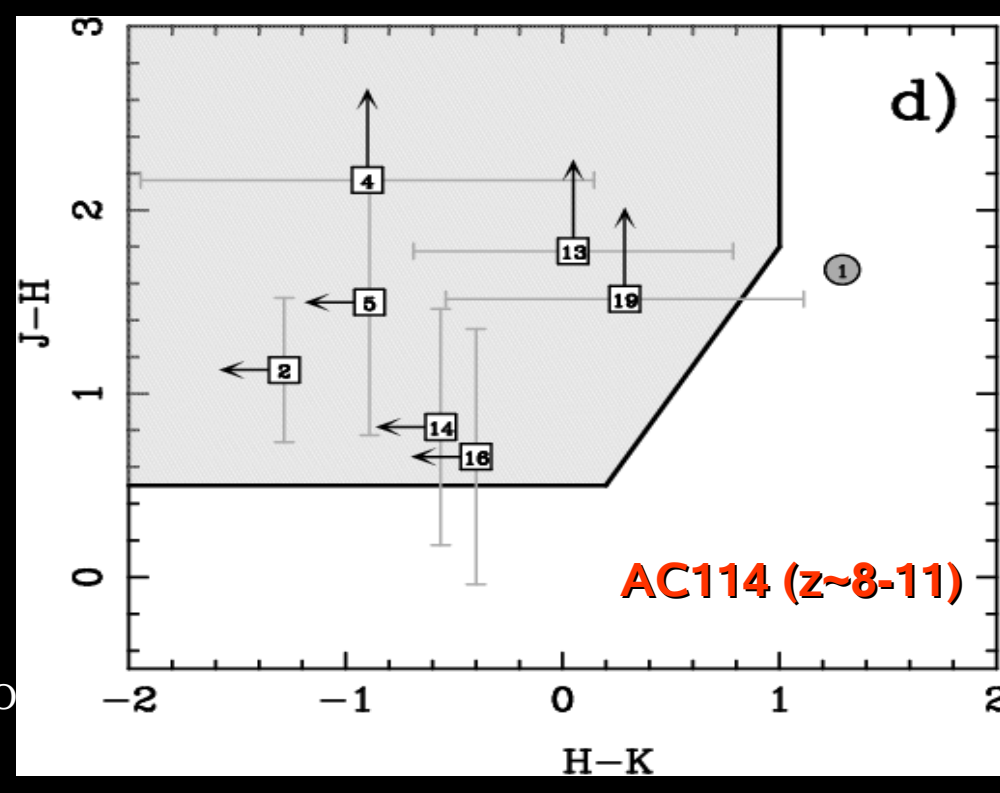
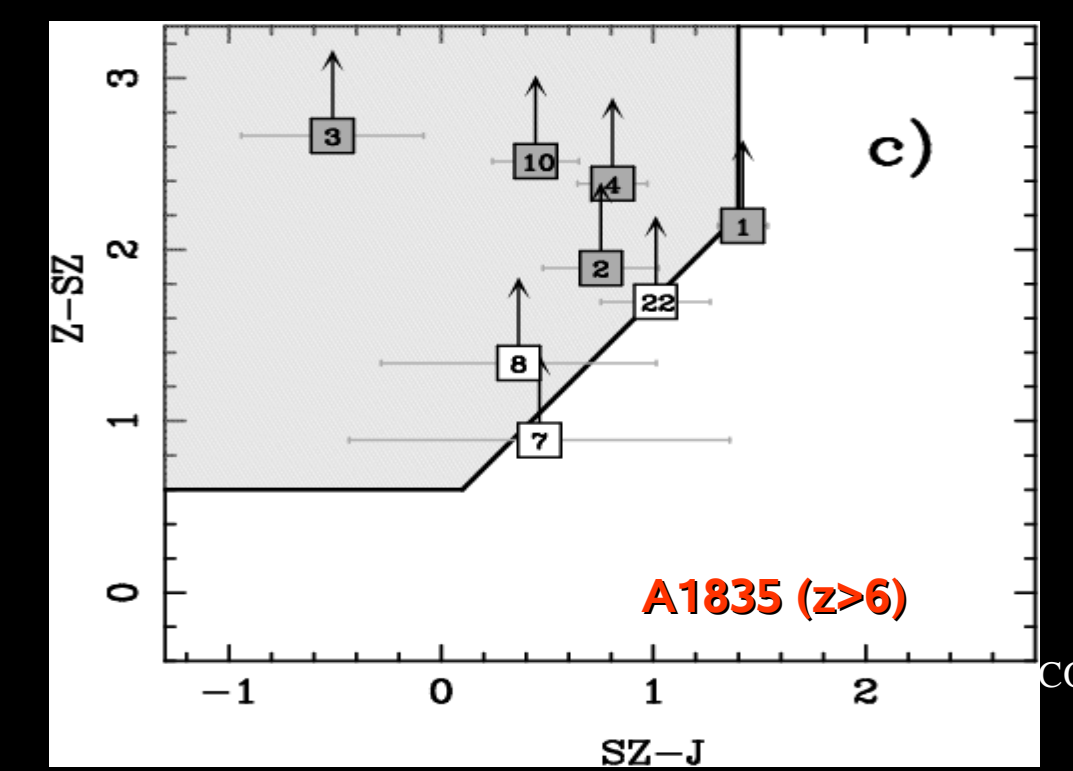
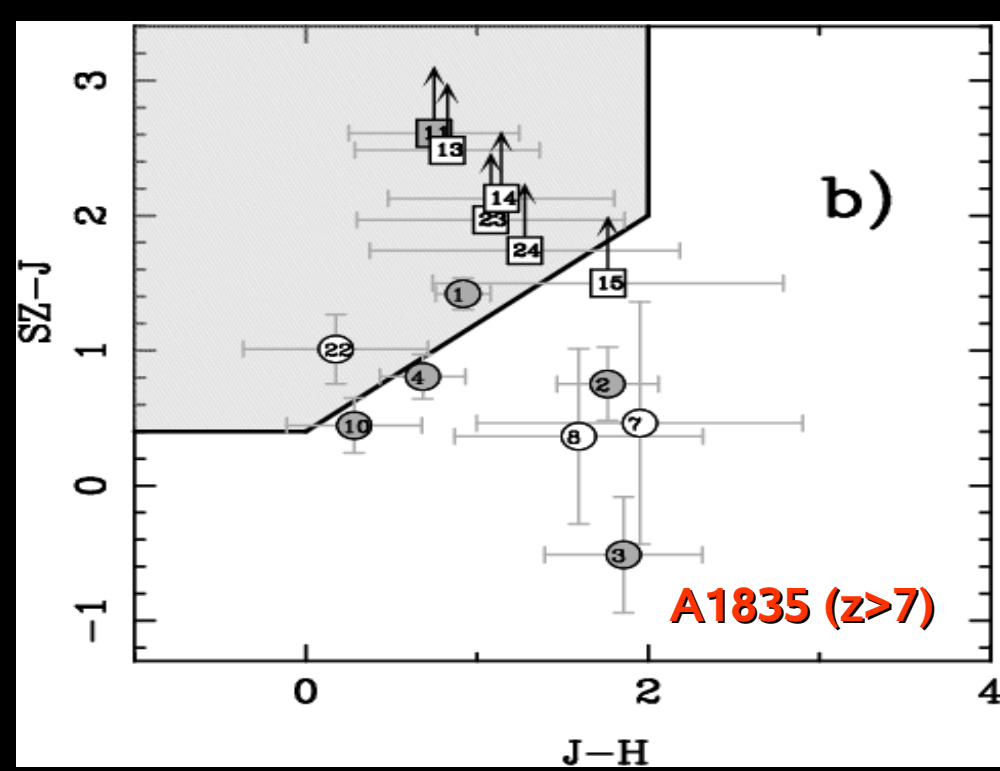
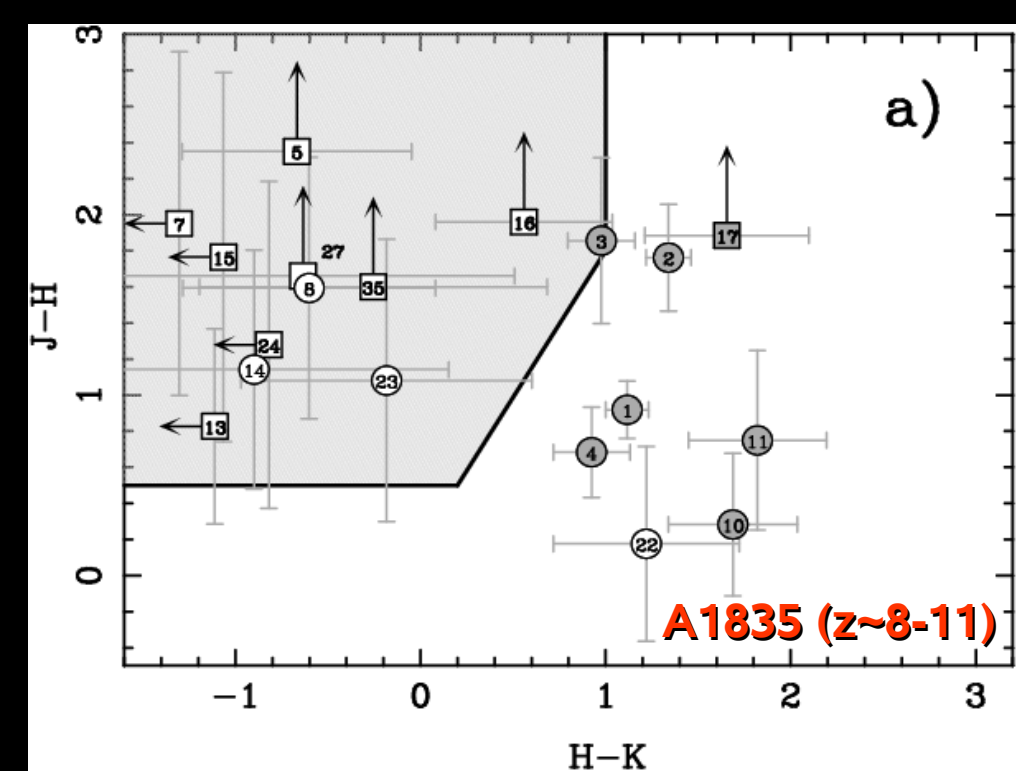
H : 4h (H = 23.5)

K': 5.5 h (K' = 23.6 --> K(AB)=25.4) +

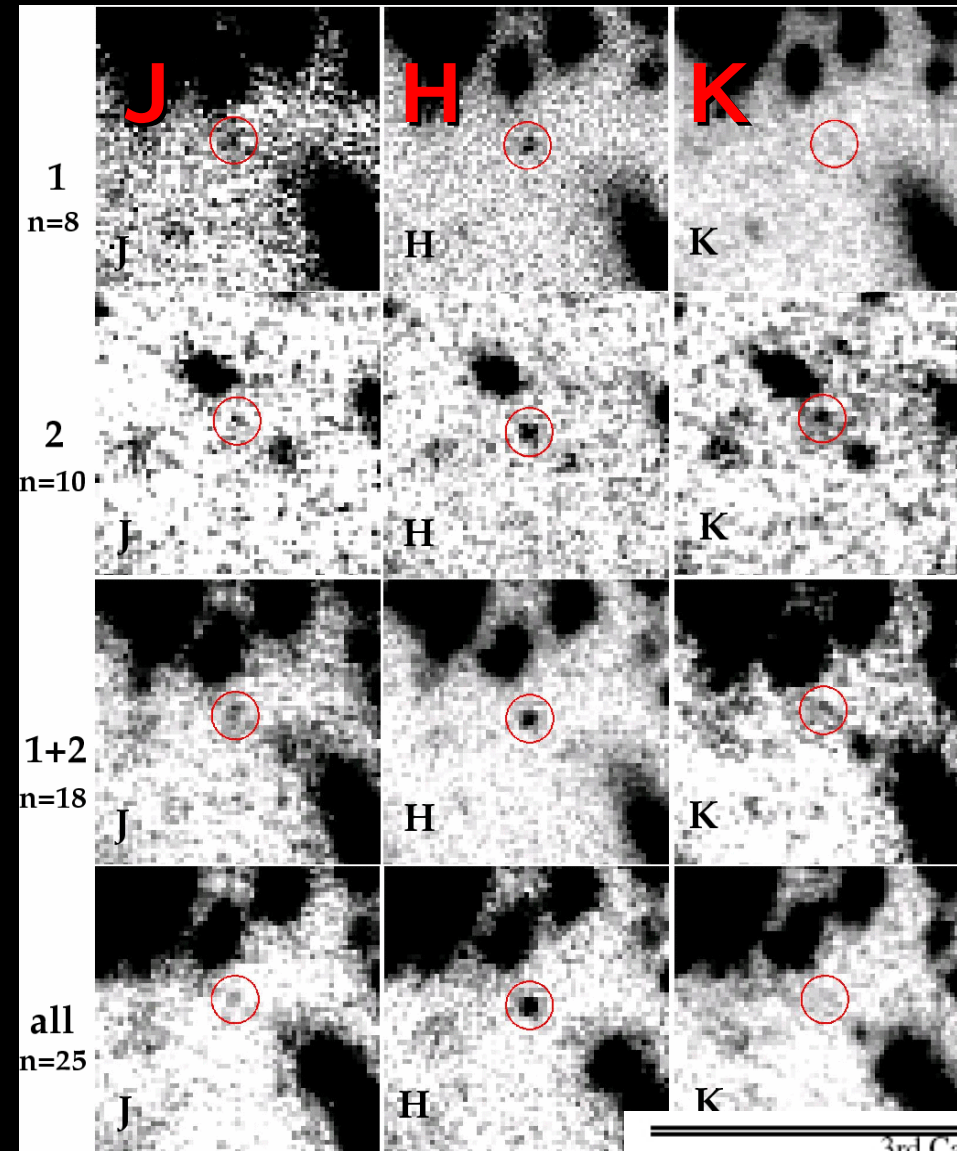
z/FORS (z=25.5) + SZ (Z=25.7)

seeing ~0.4-0.6"

+ VRI Optical data + HST R band



Stacked images of high-z candidates



- 18(8) first & second-category candidates in A1835(AC114)

CORRECTIONS:

- Lensing:

$$\eta(H_e, z) = \frac{N_o(H_e, z)}{N(H_e, z)}$$

= observed number counts up to He/
number counts in a blank field (same
depth and FOV)

$$\begin{aligned} \eta(H_e, z) &= \frac{\int_{\Delta\Omega} \frac{N(H_e, z)}{M(\Omega, z)} C(H_o) d\Omega}{\int_{\Delta\Omega} N(H_e, z) d\Omega} = \\ &= \frac{1}{\Delta\Omega} \int_{\Delta\Omega} \frac{C(H_e - 2.5 \log_{10} M(\Omega, z))}{M(\Omega, z)} d\Omega \end{aligned}$$

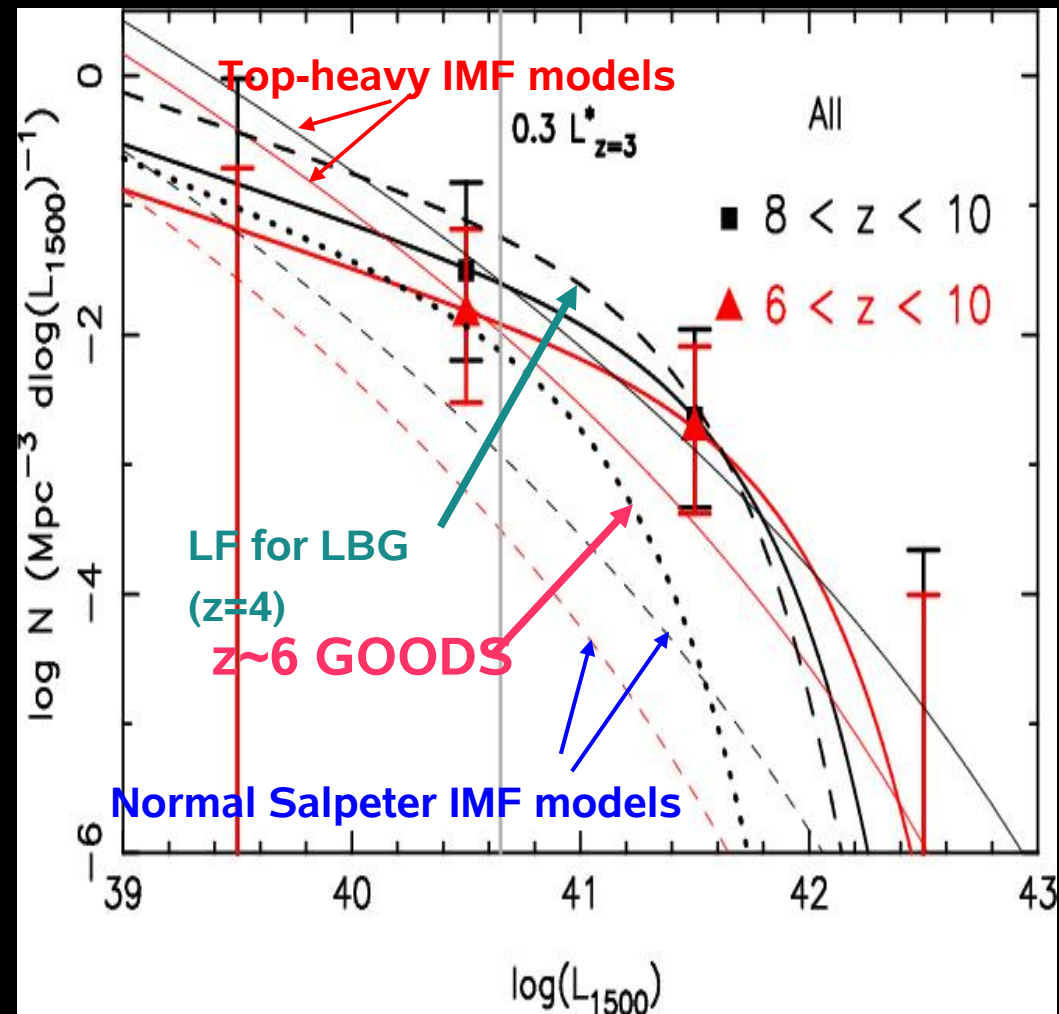
- Photometric incompleteness
- False positive detections (depending on the detection filters)
- 20-25% mid-z contamination expected

07/09/08

| H range [mag] | 3rd Cat. H | First/second category dropouts | | | | | | |
|---------------|---------------|--------------------------------|----------|----------|--------|----------|--------|----------|
| | | SZ+H | J+H | H+K | SZ+J+H | J+H+K | SZ+H+K | SZ+J+H+K |
| 22.75–23.00 | 0 (0) | 0 | 0 (0) | 0 (0) | 0 | 0 (0) | 0 | 0 |
| 23.00–23.30 | 35 (57) | 27 | 12 (25) | 25 (33) | 12 | 12 (33) | 12 | 12 |
| 23.30–23.75 | 98 (100) | 66 | 65 (88) | 61 (61) | 28 | 27 (38) | 30 | 12 |
| 23.75–24.00 | 100 (100) | 56 | 96 (100) | 73 (100) | 27 | 28 (100) | 40 | 11 |

Luminosity Functions

- Correction for lensing effects and incompleteness using the lensing model:



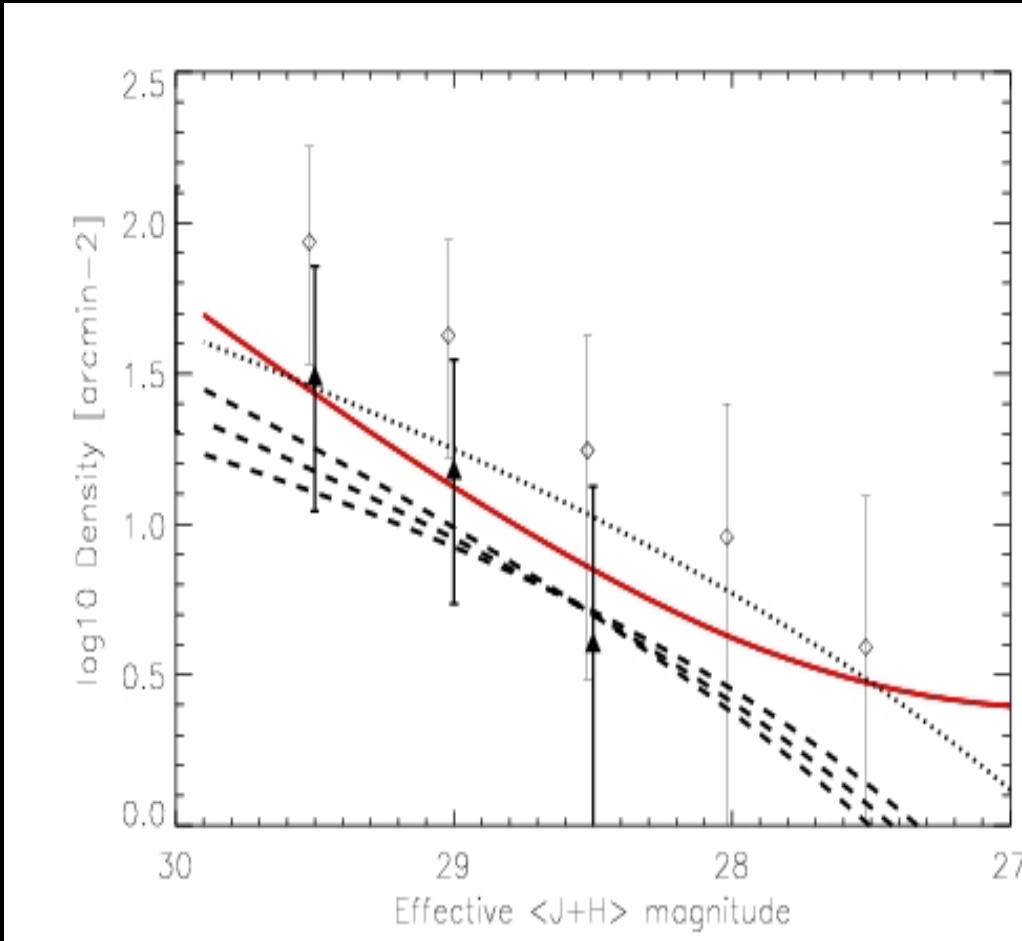
Richard et al. 06

07/09/08

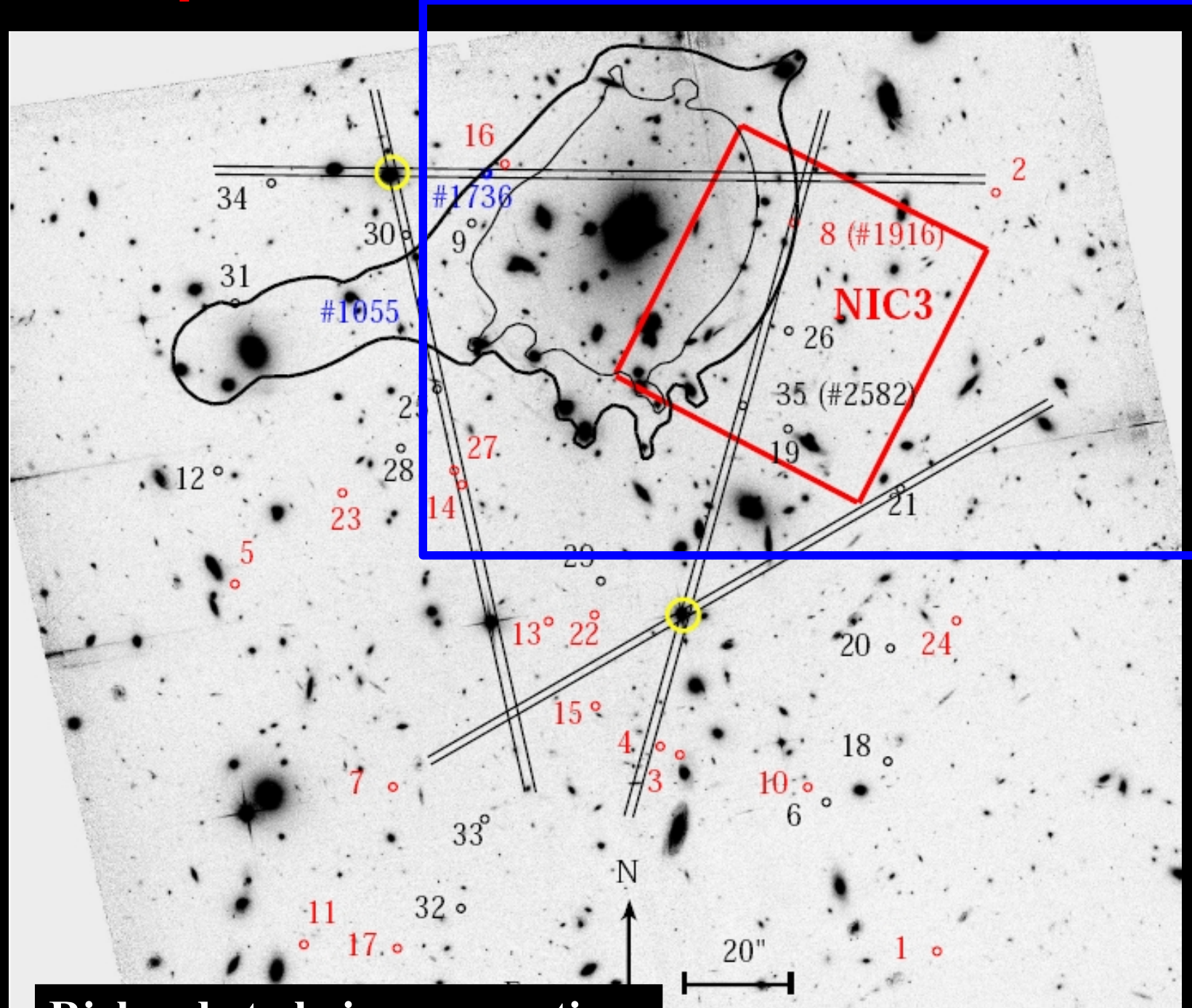
XXIVth IAP CONFERENCE

Richard et al. 08

25



Spectroscopic & Photometric follow-up



| ID | RA (14:) | DEC (02:) | SZ | J | H | K |
|--------------------------|-------------|--------------|------------------|------------------|------------------|------------------|
| First-category dropouts | | | | | | |
| #1 | 0:58.278 | 50:26.65 | 24.56 ± 0.18 | 23.14 ± 0.11 | 22.22 ± 0.10 | 21.10 ± 0.04 |
| #2 | 0:57.538 | 52:49.85 | 24.80 ± 0.22 | 24.05 ± 0.27 | 22.29 ± 0.11 | 20.95 ± 0.03 |
| #3 | 1:01.484 | 51:03.63 | 24.03 ± 0.11 | 24.54 ± 0.42 | 22.69 ± 0.16 | 21.71 ± 0.07 |
| #4 | 1:01.733 | 51:05.26 | 24.31 ± 0.14 | 23.50 ± 0.16 | 22.82 ± 0.18 | 21.90 ± 0.08 |
| #5 | 1:07.034 | 51:35.71 | 25.82 ± 0.52 | > 25.60 | 23.24 ± 0.28 | 23.91 ± 0.55 |
| #7 | 1:05.067 | 50:57.52 | 25.81 ± 0.51 | 25.34 ± 0.89 | 23.39 ± 0.32 | > 24.70 |
| #8 | 1:00.058 | 52:44.08 | 25.36 ± 0.34 | 24.99 ± 0.64 | 23.40 ± 0.32 | 24.00 ± 0.60 |
| #10 | 0:59.890 | 50:57.59 | 24.18 ± 0.12 | 23.74 ± 0.20 | 23.45 ± 0.33 | 21.77 ± 0.07 |
| #11 | 1:06.182 | 50:27.74 | > 26.90 | 24.29 ± 0.33 | 23.54 ± 0.36 | 21.72 ± 0.07 |
| #13 | 1:03.125 | 51:28.81 | > 26.90 | 24.41 ± 0.38 | 23.58 ± 0.38 | > 24.70 |
| #14 | 1:04.209 | 51:54.55 | > 26.90 | 24.77 ± 0.52 | 23.63 ± 0.39 | 24.53 ± 0.97 |
| #15 | 1:02.540 | 51:12.84 | > 26.90 | 25.40 ± 0.94 | 23.63 ± 0.40 | > 24.70 |
| #16 | 1:03.657 | 52:54.83 | > 26.90 | > 25.60 | 23.64 ± 0.40 | 23.08 ± 0.25 |
| #17 | 1:05.013 | 50:27.11 | > 26.90 | > 25.60 | 23.71 ± 0.43 | 22.06 ± 0.10 |
| #22 | 1:02.551 | 51:30.06 | 25.00 ± 0.24 | 23.99 ± 0.25 | 23.81 ± 0.47 | 22.59 ± 0.16 |
| #23 | 1:05.699 | 51:52.92 | > 26.90 | 24.93 ± 0.61 | 23.85 ± 0.48 | 24.03 ± 0.61 |
| #24 | 0:58.036 | 51:29.09 | > 26.90 | 25.16 ± 0.75 | 23.88 ± 0.50 | > 24.70 |
| #27 | 1:04.299 | 51:57.19 | > 26.90 | > 25.60 | 23.93 ± 0.53 | 24.57 ± 1.01 |
| Second-category dropouts | | | | | | |
| #6 | 0:59.659 | 50:54.73 | > 26.90 | > 25.60 | 23.37 ± 0.31 | > 24.70 |
| #18 | 0:58.890 | 51:02.47 | > 26.90 | > 25.60 | 23.72 ± 0.43 | > 24.70 |
| #19 | 1:00.138 | 52:05.20 | > 26.90 | > 25.60 | 23.72 ± 0.43 | > 24.70 |
| #20 | 0:58.860 | 51:23.85 | > 26.90 | > 25.60 | 23.72 ± 0.43 | > 24.70 |
| #21 | 0:58.732 | 51:53.86 | > 26.90 | > 25.60 | 23.76 ± 0.44 | > 24.70 |
| #35 | 1:00.693 | 52:09.58 | > 26.90 | > 25.60 | 24.00 ± 0.56 | 24.25 ± 0.75 |

• Mid-z EROs

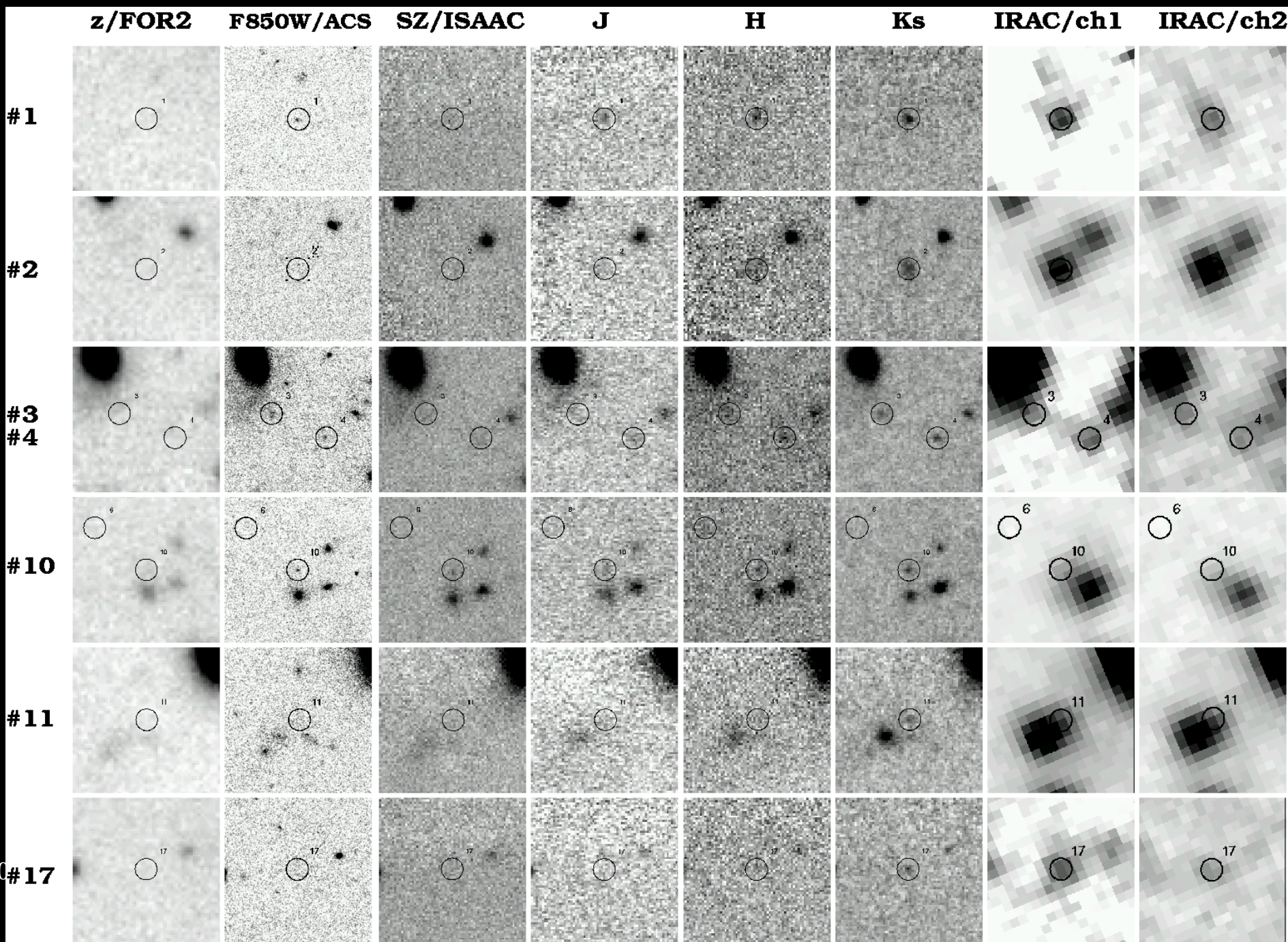
• Excluded from LF analysis in Richard et al. 06

• IRAC sources

• Multi-wavelength analysis by Schaerer et al. 07

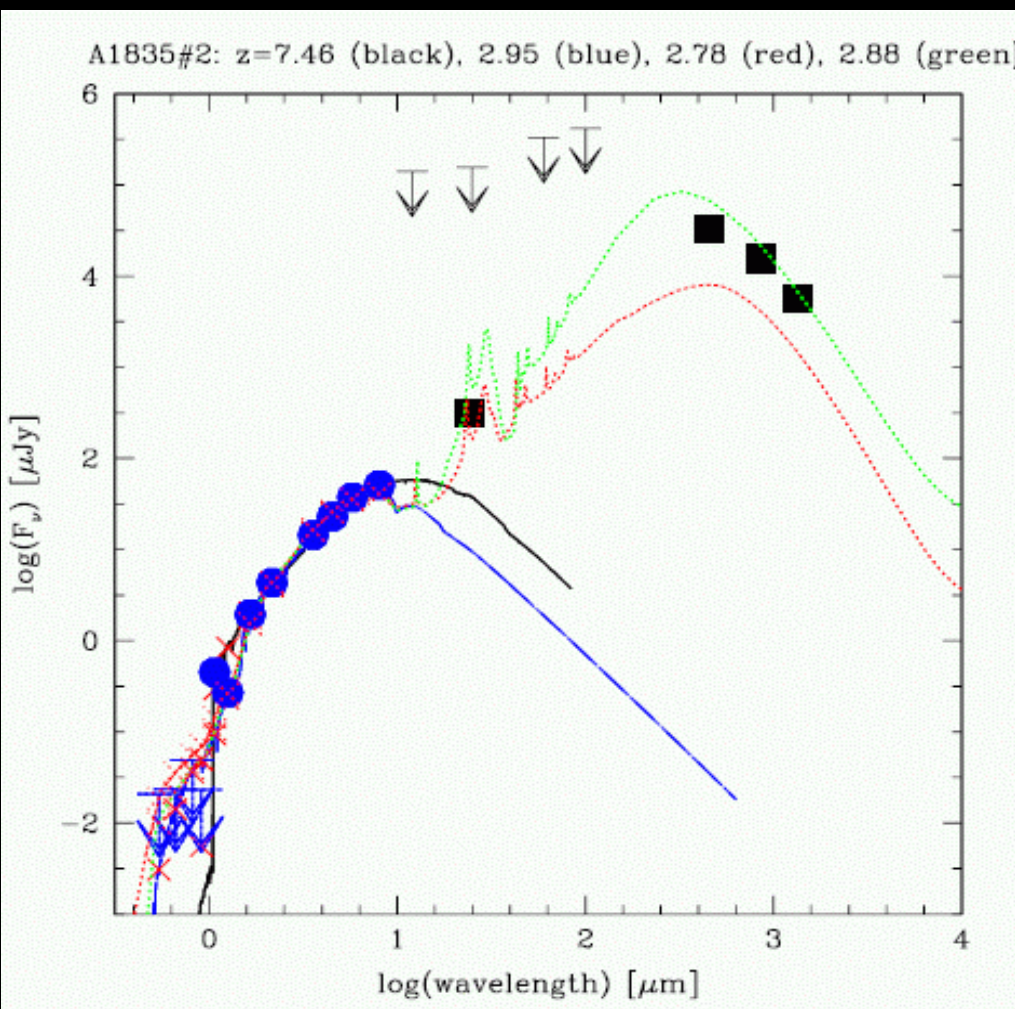
Multi-wavelength analysis

«Bright» optical dropouts in A1835

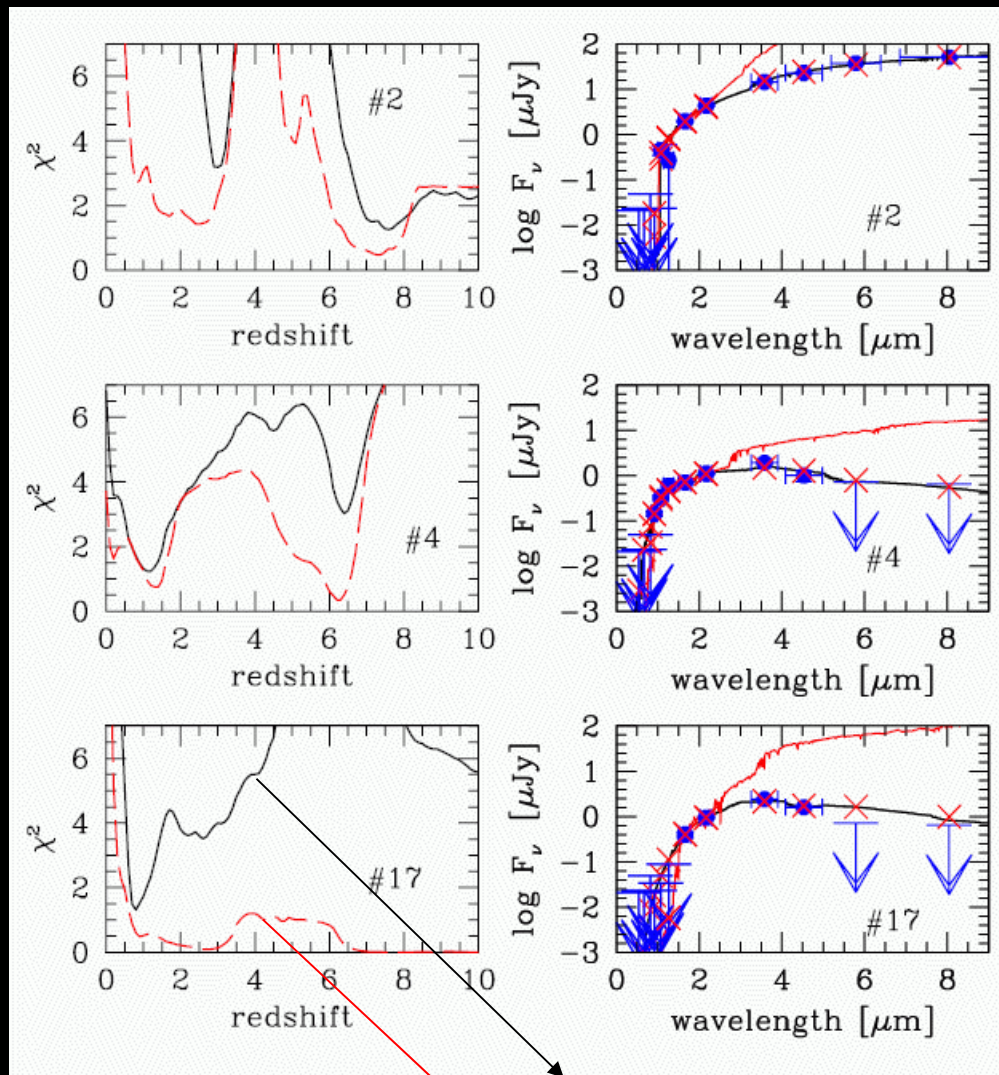


- **IRAC/Spitzer :**

- Detection of brightest objects (ERO) between 3.8 and 8 μm --> new constraints on their nature and redshift
- high-z candidates not detected as expected



ACS/HST z-band observations (non-detection $Z850_{\text{AB}} > 28.$ to 28.3) confirm « dropout » nature of $z > \sim 7$ candidates behind A1835 and AC114.



INFERENCE

(Schaefer et al. 07, Hempel et al. 08)

with IRAC data
without IRAC data

| ID | RA (14:) | DEC (02:) | <i>SZ</i> | <i>J</i> | <i>H</i> | <i>K</i> |
|--------------------------|-------------|--------------|------------------|------------------|------------------|------------------|
| First-category dropouts | | | | | | |
| #1 | 0:58.278 | 50:26.65 | 24.56 ± 0.18 | 23.14 ± 0.11 | 22.22 ± 0.10 | 21.10 ± 0.04 |
| #2 | 0:57.538 | 52:49.85 | 24.80 ± 0.22 | 24.05 ± 0.27 | 22.29 ± 0.11 | 20.95 ± 0.03 |
| #3 | 1:01.484 | 51:03.63 | 24.03 ± 0.11 | 24.54 ± 0.42 | 22.69 ± 0.16 | 21.71 ± 0.07 |
| #4 | 1:01.733 | 51:05.26 | 24.31 ± 0.14 | 23.50 ± 0.16 | 22.82 ± 0.18 | 21.90 ± 0.08 |
| #5 | 1:07.034 | 51:35.71 | 25.82 ± 0.52 | > 25.60 | 23.24 ± 0.28 | 23.01 ± 0.55 |
| #7 | 1:05.037 | 50:57.52 | 25.81 ± 0.51 | 25.34 ± 0.89 | 23.09 ± 0.32 | > 24.70 |
| #8 | 1:00.058 | 52:44.08 | 25.36 ± 0.34 | 24.99 ± 0.64 | 23.40 ± 0.32 | 24.00 ± 0.60 |
| #10 | 0:59.890 | 50:57.59 | 24.18 ± 0.12 | 23.74 ± 0.20 | 23.45 ± 0.33 | 21.77 ± 0.07 |
| #11 | 1:06.182 | 50:27.74 | > 26.90 | 24.29 ± 0.33 | 23.54 ± 0.36 | 21.72 ± 0.07 |
| #13 | 1:03.125 | 51:28.81 | > 26.90 | 24.41 ± 0.38 | 23.58 ± 0.38 | > 24.70 |
| #14 | 1:04.209 | 51:54.55 | > 26.90 | 24.77 ± 0.52 | 23.63 ± 0.39 | 24.53 ± 0.97 |
| #15 | 1:02.540 | 51:12.84 | > 26.90 | 25.40 ± 0.94 | 23.63 ± 0.40 | > 24.70 |
| #16 | 1:03.657 | 52:54.83 | > 26.90 | > 25.60 | 23.64 ± 0.40 | 23.08 ± 0.25 |
| #17 | 1:05.013 | 50:27.11 | > 26.90 | > 25.60 | 23.71 ± 0.43 | 22.06 ± 0.10 |
| #22 | 1:02.551 | 51:30.06 | 25.00 ± 0.24 | 23.99 ± 0.25 | 23.81 ± 0.47 | 22.59 ± 0.16 |
| #23 | 1:05.699 | 51:52.92 | > 26.90 | 24.93 ± 0.61 | 23.85 ± 0.48 | 24.03 ± 0.61 |
| #24 | 0:58.036 | 51:29.09 | > 26.90 | 25.16 ± 0.75 | 23.88 ± 0.50 | > 24.70 |
| #27 | 1:04.299 | 51:57.19 | > 26.90 | > 25.60 | 23.93 ± 0.53 | 24.57 ± 1.01 |
| Second-category dropouts | | | | | | |
| #6 | 0:59.659 | 50:54.73 | > 26.90 | > 25.60 | 23.37 ± 0.31 | > 24.70 |
| #18 | 0:58.890 | 51:02.47 | > 26.90 | > 25.60 | 23.72 ± 0.43 | > 24.70 |
| #19 | 1:00.138 | 52:05.20 | > 26.90 | > 25.60 | 23.72 ± 0.43 | > 24.70 |
| #20 | 0:58.860 | 51:23.85 | > 26.90 | > 25.60 | 23.72 ± 0.43 | > 24.70 |
| #21 | 0:58.732 | 51:53.86 | > 26.90 | > 25.60 | 23.76 ± 0.44 | > 24.70 |
| #35 | 1:00.693 | 52:09.58 | > 26.90 | > 25.60 | 24.00 ± 0.56 | 24.25 ± 0.75 |

X

X

X

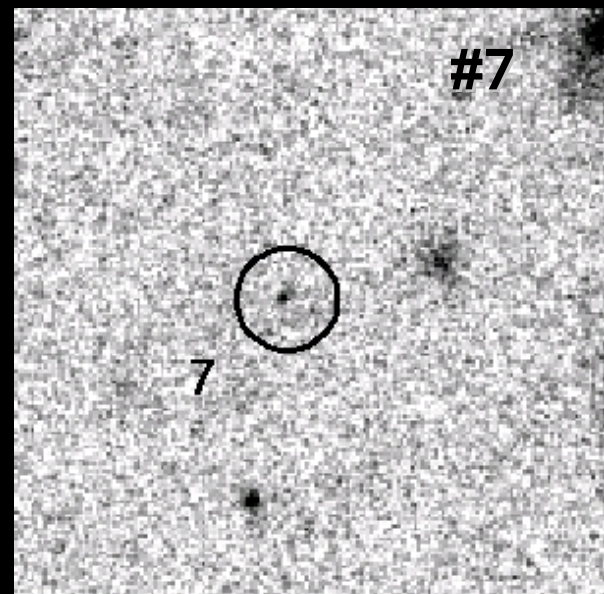
?

X

?

- Detected on ACS/F850 image

- Confirmation of optical dropout



#31

#32

| ID | RA (14:) | DEC (02:) | SZ | J | H | K |
|--------------------------|-------------|--------------|------------------|------------------|------------------|------------------|
| First-category dropouts | | | | | | |
| #1 | 0:58.278 | 50:26.65 | 24.56 ± 0.18 | 23.14 ± 0.11 | 22.22 ± 0.10 | 21.10 ± 0.04 |
| #2 | 0:57.538 | 52:49.85 | 24.80 ± 0.22 | 24.05 ± 0.27 | 22.29 ± 0.11 | 20.95 ± 0.03 |
| #3 | 1:01.484 | 51:03.63 | 24.03 ± 0.11 | 24.54 ± 0.42 | 22.69 ± 0.16 | 21.71 ± 0.07 |
| #4 | 1:01.733 | 51:05.26 | 24.31 ± 0.14 | 23.50 ± 0.16 | 22.82 ± 0.18 | 21.90 ± 0.08 |
| #5 | 1:07.034 | 51:35.71 | 25.82 ± 0.52 | > 25.60 | 23.24 ± 0.28 | 23.01 ± 0.55 |
| #7 | 1:05.037 | 50:57.52 | 25.81 ± 0.51 | 25.34 ± 0.89 | 23.09 ± 0.32 | > 24.70 |
| #8 | 1:00.058 | 52:44.08 | 25.36 ± 0.34 | 24.99 ± 0.64 | 23.40 ± 0.32 | 24.00 ± 0.60 |
| #10 | 0:59.890 | 50:57.59 | 24.18 ± 0.12 | 23.74 ± 0.20 | 23.45 ± 0.33 | 21.77 ± 0.07 |
| #11 | 1:06.182 | 50:27.74 | > 26.90 | 24.29 ± 0.33 | 23.54 ± 0.36 | 21.72 ± 0.07 |
| #13 | 1:03.125 | 51:28.81 | > 26.90 | 24.41 ± 0.38 | 23.58 ± 0.38 | > 24.70 |
| #14 | 1:04.209 | 51:54.55 | > 26.90 | 24.77 ± 0.52 | 23.63 ± 0.39 | 24.53 ± 0.97 |
| #15 | 1:02.540 | 51:12.84 | > 26.90 | 25.40 ± 0.94 | 23.63 ± 0.40 | > 24.70 |
| #16 | 1:03.657 | 52:54.83 | > 26.90 | > 25.60 | 23.64 ± 0.40 | 23.08 ± 0.25 |
| #17 | 1:05.013 | 50:27.11 | > 26.90 | > 25.60 | 23.71 ± 0.43 | 22.06 ± 0.10 |
| #22 | 1:02.551 | 51:30.06 | 25.00 ± 0.24 | 23.99 ± 0.25 | 23.81 ± 0.47 | 22.59 ± 0.16 |
| #23 | 1:05.699 | 51:52.92 | > 26.90 | 24.93 ± 0.61 | 23.85 ± 0.48 | 24.03 ± 0.61 |
| #24 | 0:58.656 | 51:29.59 | > 26.90 | 25.16 ± 0.75 | 23.88 ± 0.50 | > 24.70 |
| #27 | 1:04.299 | 51:57.19 | > 26.90 | > 25.60 | 23.93 ± 0.53 | 24.57 ± 1.01 |
| Second-category dropouts | | | | | | |
| #6 | 0:59.659 | 50:54.73 | > 26.90 | > 25.60 | 23.37 ± 0.31 | > 24.70 |
| #18 | 0:58.890 | 51:02.47 | > 26.90 | > 25.60 | 23.72 ± 0.43 | > 24.70 |
| #19 | 1:00.138 | 52:05.20 | > 26.90 | > 25.60 | 23.72 ± 0.43 | > 24.70 |
| #20 | 0:58.860 | 51:23.85 | > 26.90 | > 25.60 | 23.72 ± 0.43 | > 24.70 |
| #21 | 0:58.732 | 51:53.86 | > 26.90 | > 25.60 | 23.76 ± 0.44 | > 24.70 |
| #35 | 1:00.693 | 52:09.58 | > 26.90 | > 25.60 | 24.00 ± 0.56 | 24.25 ± 0.75 |

X

X

X ?

X

X X

? X

? X

X

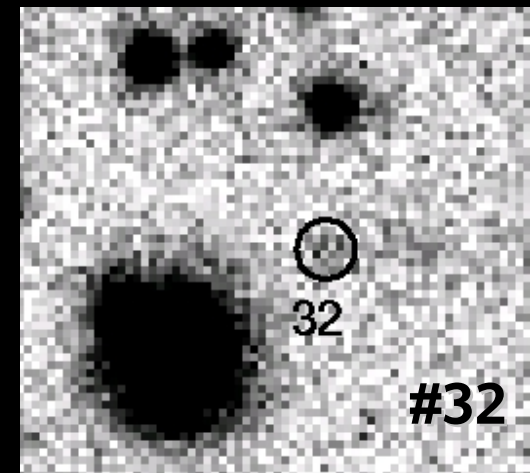
X X

? X

X

- Detected on FORS/V image

- Mid-z interlopers



#31

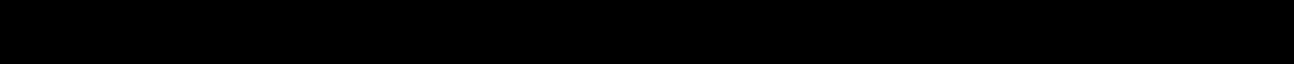
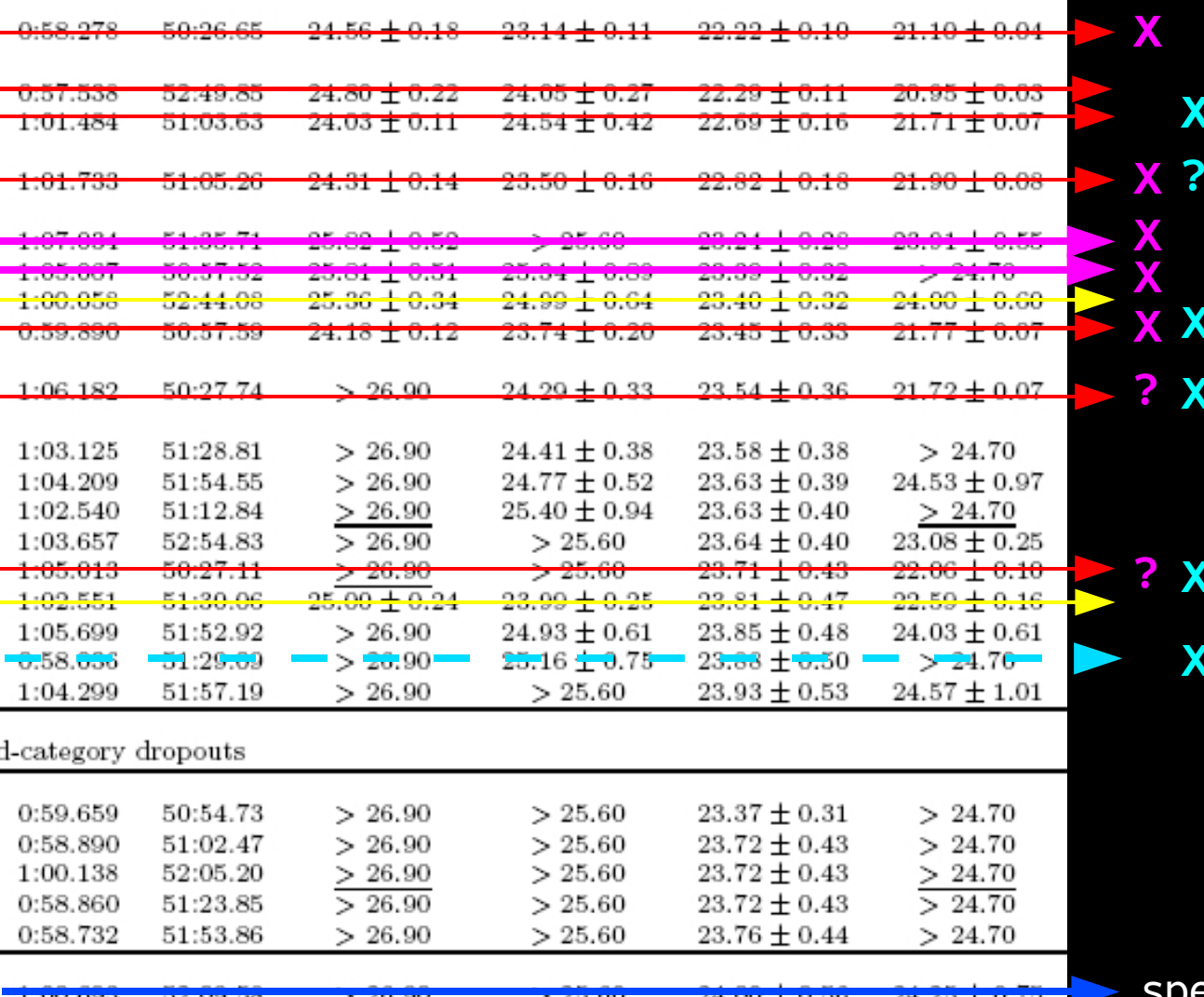
#32

#26

#32

ACS/F850 - FORS/V

| ID | RA (14:) | DEC (02:) | SZ | J | H | K |
|--------------------------|-------------|--------------|------------------|------------------|------------------|------------------|
| First-category dropouts | | | | | | |
| #1 | 0:58.278 | 50:26.65 | 24.56 ± 0.18 | 23.11 ± 0.11 | 22.22 ± 0.10 | 21.10 ± 0.04 |
| #2 | 0:57.538 | 52:49.85 | 24.80 ± 0.22 | 24.05 ± 0.27 | 22.29 ± 0.11 | 20.95 ± 0.03 |
| #3 | 1:01.484 | 51:03.63 | 24.03 ± 0.11 | 24.54 ± 0.42 | 22.69 ± 0.16 | 21.71 ± 0.07 |
| #4 | 1:01.733 | 51:05.26 | 24.31 ± 0.14 | 23.50 ± 0.16 | 22.82 ± 0.18 | 21.90 ± 0.08 |
| #5 | 1:07.034 | 51:35.71 | 25.82 ± 0.52 | > 25.60 | 23.24 ± 0.28 | 23.01 ± 0.55 |
| #7 | 1:05.037 | 50:57.52 | 25.81 ± 0.51 | 25.34 ± 0.89 | 23.09 ± 0.32 | > 24.70 |
| #8 | 1:00.058 | 52:44.08 | 25.36 ± 0.34 | 24.99 ± 0.64 | 23.46 ± 0.32 | 24.00 ± 0.60 |
| #10 | 0:59.890 | 50:57.59 | 24.18 ± 0.12 | 23.74 ± 0.20 | 23.45 ± 0.33 | 21.77 ± 0.07 |
| #11 | 1:06.182 | 50:27.74 | > 26.90 | 24.29 ± 0.33 | 23.54 ± 0.36 | 21.72 ± 0.07 |
| #13 | 1:03.125 | 51:28.81 | > 26.90 | 24.41 ± 0.38 | 23.58 ± 0.38 | > 24.70 |
| #14 | 1:04.209 | 51:54.55 | > 26.90 | 24.77 ± 0.52 | 23.63 ± 0.39 | 24.53 ± 0.97 |
| #15 | 1:02.540 | 51:12.84 | > 26.90 | 25.40 ± 0.94 | 23.63 ± 0.40 | > 24.70 |
| #16 | 1:03.657 | 52:54.83 | > 26.90 | > 25.60 | 23.64 ± 0.40 | 23.08 ± 0.25 |
| #17 | 1:05.013 | 50:27.11 | > 26.90 | > 25.60 | 23.71 ± 0.43 | 22.06 ± 0.10 |
| #22 | 1:02.551 | 51:30.06 | 25.00 ± 0.24 | 23.99 ± 0.25 | 23.81 ± 0.47 | 22.59 ± 0.16 |
| #23 | 1:05.699 | 51:52.92 | > 26.90 | 24.93 ± 0.61 | 23.85 ± 0.48 | 24.03 ± 0.61 |
| #24 | 0:58.656 | 51:29.69 | > 26.90 | 25.16 ± 0.75 | 23.88 ± 0.50 | > 24.70 |
| #27 | 1:04.299 | 51:57.19 | > 26.90 | > 25.60 | 23.93 ± 0.53 | 24.57 ± 1.01 |
| Second-category dropouts | | | | | | |
| #6 | 0:59.659 | 50:54.73 | > 26.90 | > 25.60 | 23.37 ± 0.31 | > 24.70 |
| #18 | 0:58.890 | 51:02.47 | > 26.90 | > 25.60 | 23.72 ± 0.43 | > 24.70 |
| #19 | 1:00.138 | 52:05.20 | > 26.90 | > 25.60 | 23.72 ± 0.43 | > 24.70 |
| #20 | 0:58.860 | 51:23.85 | > 26.90 | > 25.60 | 23.72 ± 0.43 | > 24.70 |
| #21 | 0:58.732 | 51:53.86 | > 26.90 | > 25.60 | 23.76 ± 0.44 | > 24.70 |
| #35 | 1:00.693 | 52:09.56 | > 26.90 | > 25.60 | 24.00 ± 0.50 | 24.25 ± 0.75 |



- Robust SZ(Y) re-detections
- Among the 1rst rank candidates, #8, #14, #16, #27 are not (re)dected in NIRI or NIC3.
- #35 (spectroscopy!) & #26 (low-z) are real, but not (re)dected in NIRI or NIC3!
- High contamination by stars & mid-z interlopers: 10/35 dropouts; ~1/4 of faint high-z candidates

spectroscopic confirmation $z=1.67$

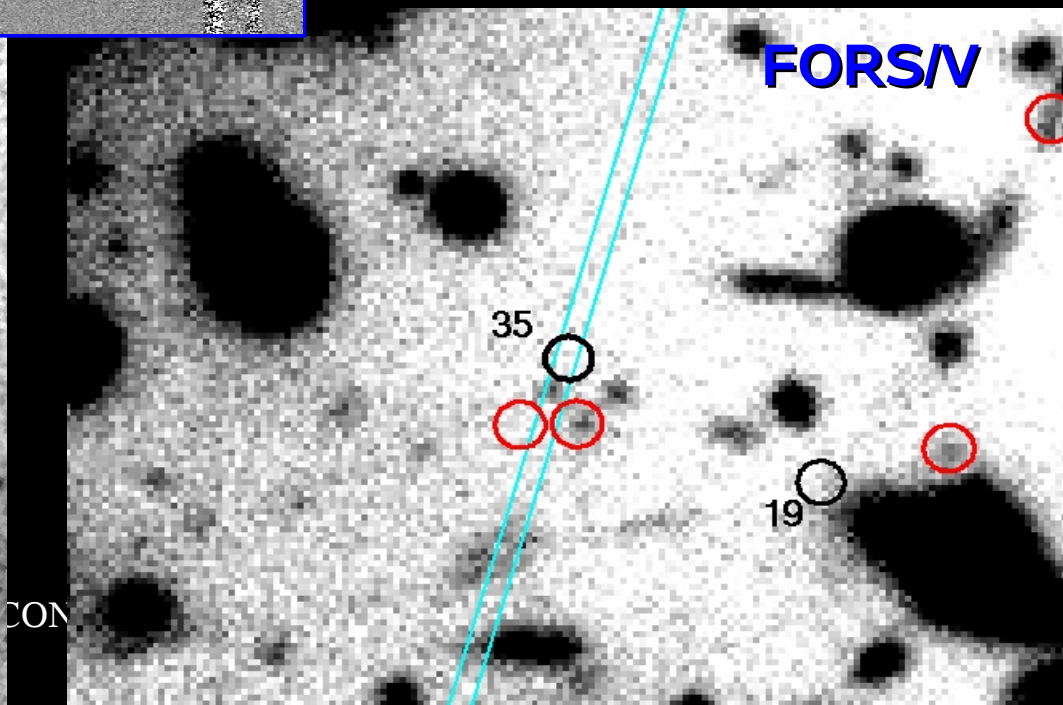
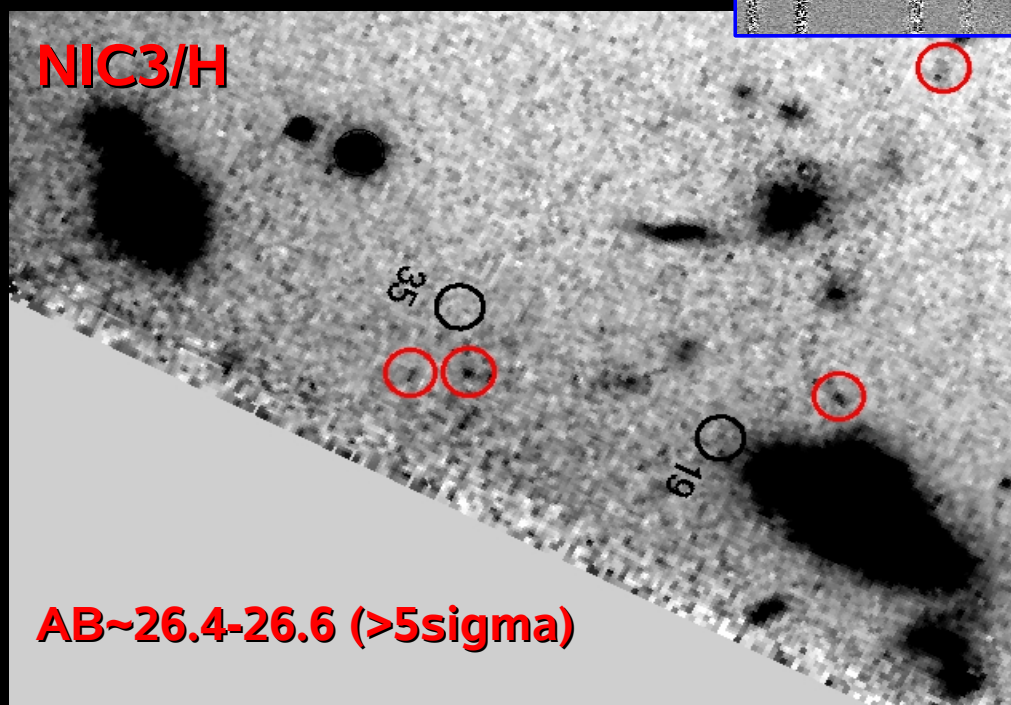
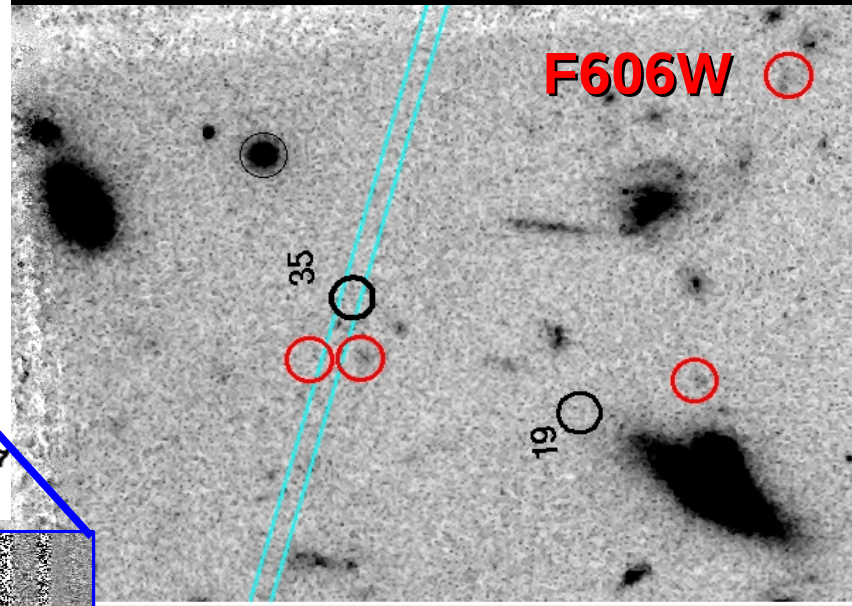
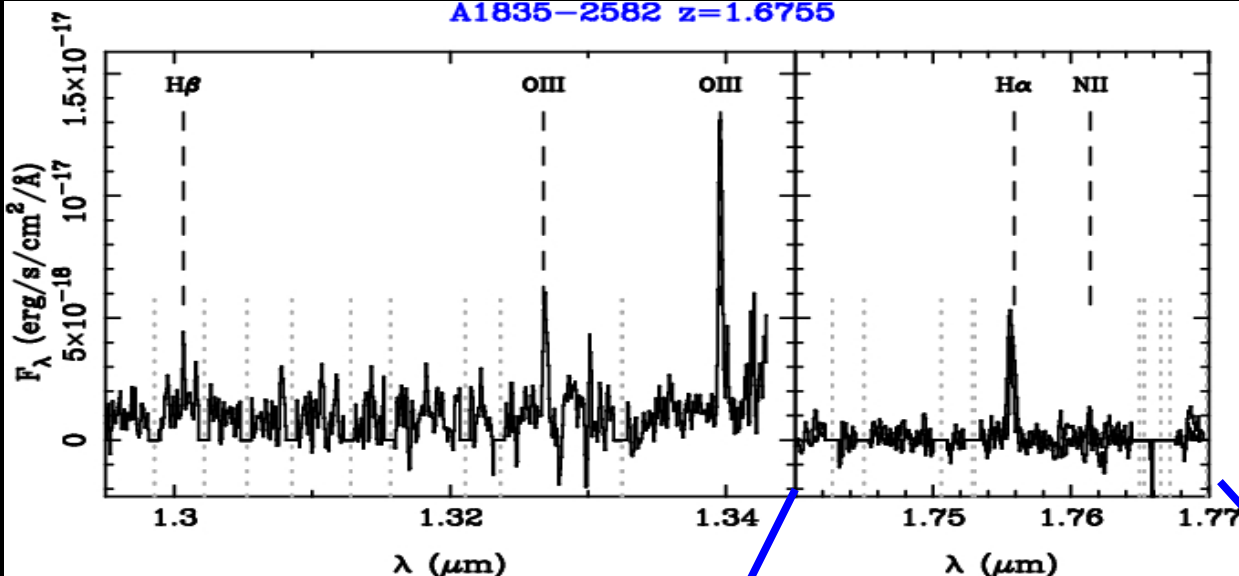
X X

? X

X

A puzzling source: A1835#135

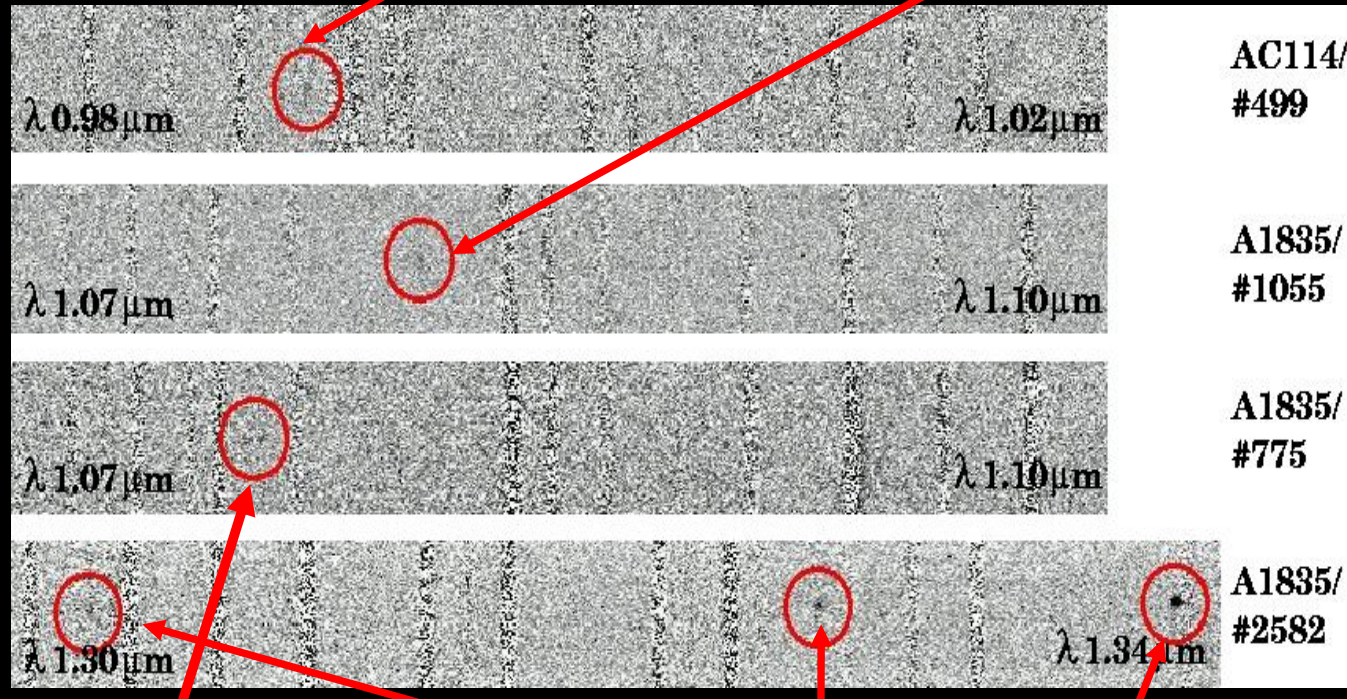
A1835-2582 z=1.6755



Spectroscopic follow-up

$z=7.17$ candidate if Ly α

$z=7.89$ Candidate if Ly α



$z=1.89$, doublet of [OII]3727

$z=1.67$, 3 lines detected
(Richard et al. 2003)

A tedious and highly inefficient process with ISAAC/VLT...

Targets: 2 priority candidates in AC114, and 7 in Abell 1835 (4 ``first priority'' targets and 3 secondary ones). From this sample of 9 targets, 2/3 of the objects observed display emission lines.

- A large majority of our high-z candidates still need to be (re)confirmed, either by a re-detection of a faint emission line, or by the non-detection of other lines expected at low-z.
- FORS/VLT z-band spectra on the “bright” EROs.

Summary/Conclusions

- Gravitational lensing clusters are more efficient than blank fields to explore the z~6-7 to 12 domain (same photometric depth and FOV). A significant positive magnification bias expected:
 - for “shallow” surveys/ small FOV
 - increasing for “pessimistic” (or strongly evolving) LFs
 - increasing with z(sources)
- The comparison between $N(z,m)$ in (different) lensing and blank fields helps constraining the faint end of LF.
- Spectroscopic follow up optimized in lensing fields with the new generation of near-IR multi-object spectrographs (FOV, multiplexing and spectral resolution).
- Large field-to-field variance in the strong magnification regime and towards the bright end of the LF ==> Wide Field Surveys are also needed.
- First lensing results at $6 < z < 10$ were consistent with a ~constant SFR density up to $z \sim 10$. The turnover towards the bright end of the LF is not observed. However:
 - > *strong field-to-field variance*
 - > *large corrections have been applied to relatively small samples*
 - > *low-z contamination (with respect to blank fields) could be higher than expected*
==> **spectroscopic/photometric confirmation is needed**



Thanks!